EXAMINATION OF SPECIFIC AMINO ACID RESIDUES OF *DESULFOVIBRIO DESULFURICANS* CYTOCHROME C_3 IN ELECTRON TRANSFER

A Thesis

presented to

The Faculty of the Graduate School

University of Missouri-Columbia

In Partial Fulfillment

of the Requirements for the Degree of

Master of Science

---

by

Suzanne M. Miller

Dr. Judy D. Wall, thesis supervisor

DECEMBER 2005

The undersigned, appointed by the Dean of Graduate School, have examined the thesis entitled:

EXAMINATION OF SPECIFIC AMINO ACID RESIDUES OF *DESULFOVIBRIO DESULFURICANS* CYTOCHROME C_3 IN ELECTRON TRANSFER

Presented by Suzanne M. Miller on August 5, 2005.

A candidate for the degree of Master of Science

And hereby certify that in their opinion it is worthy of acceptance.

Judy D. McCall

Mark A. McIntosh

David W. Emerich

ACKNOWLEDGMENTS

I thank my advisor Dr. Judy Wall who has provided an outstanding example as a scientist and also as a mentor. I am grateful for her enthusiasm, dedication, and incomparable support throughout my graduate education.

I thank the following members of the lab past and present: Barbara Giles, Leena Pattarkine, Rayford Payne, Grant Zane, Joseph Ringbauer, Bill Yen, Kelly Bender, Eliot Drury, Kate Hart, Christopher Hemme, Lise Larsen, Jana Thoma, and Joyce McBeth. They have given technical assistance and have made coming to work each day enjoyable.

I thank Leena Pattarkine for her contributions preceding this work, and especially for much needed guidance and patience while teaching me the protein basics.

I thank Mark Palmier for expertise and technical assistance in preparation of the antibody affinity columns.

I thank members of my committee: Dr. David Emerich, Dr. David Pintel, Dr. Karen Bennett, and Dr. Mark McIntosh for giving direction and advice.

I give great thanks to my parents, Dr. William Bruce Miller and Mrs. Patricia Miller. They have given me unconditional love and encouragement throughout my life and I am forever grateful for the opportunities given to me to pursue my education

EXAMINATION OF SPECIFIC AMINO ACID RESIDUES OF *DESULFOVIBRIO DESULFURICANS* CYTOCHROME C_3 IN ELECTRON TRANSFER

Suzanne M. Miller

Dr. Judy D. Wall, Thesis Advisor

Sulfate-reducing bacteria (SRB) are strictly anaerobic microorganisms present throughout the environment. These microorganisms are able to utilize a variety of electron donors and couple the oxidation of those compounds to the reduction of sulfate, with sulfate as the terminal electron acceptor and hydrogen sulfide as an end product of respiration. The generation of hydrogen sulfide is problematic because of its corrosive effects on metals and concrete. On the positive side, there exists the potential to utilize the metabolic properties of the bacteria for the bioremediation of toxic metals such as uranium. Many of the SRB are capable of altering the redox state of uranium from soluble U(VI) to the insoluble mineral uraninite U(IV) that is less biologically available. Of particular interest in this investigation is the involvement of the predominant c-type tetraheme cytochrome, cytochrome c_3, implicated as a metal reductase in SRB metabolic processes. To explore this possibility, a number of mutant cytochrome c_3 proteins were generated and electron transfer capabilities to metals and metal complexes were examined. UV spectroscopy was used to observe the redox properties of wild-type and mutant cytochromes with the addition of uranium and molybdate. Oxidation and reduction was observed to be similar

to non-mutant, for the mutations F19A, C45A, K66A, K72A, and M80K. However, the K14A mutant was not oxidized when molybdate was added to the reduced protein. This lysine residue may represent a critical point of interaction between the cytochrome and the metal.

LIST OF TABLES

LIST OF FIGURES

TABLE OF CONTENTS

Chapter 1

INTRODUCTION

Sulfate-reducing bacteria (SRB) are essential in the global sulfur cycle. These microorganisms are able to utilize a variety of electron donors and couple the oxidation of those compounds to the reduction of sulfate as the terminal electron acceptor for respiration. These bacteria are also capable of reducing various metals and therefore may provide an effective means for the bioremediation of toxic metals such as uranium. In the reduced state, uranium is insoluble and therefore less biologically available. The predominant *c*-type tetraheme cytochrome of the *Desulfovibrio*, cytochrome c_3, has been implicated as a metal reductase in the reduction of U(VI) to U(IV). In order to gain greater understanding of the interactions and electron transfer mechanisms a number of mutant cytochrome c_3 proteins were generated and electron transfer capabilities to metals and metal complexes were evaluated.

I. Ecological Significance

Desulfovibrio desulfuricans is characterized as a sulfate-reducing bacterium, meaning that dissimilatory suflate reduction is a distinguishing feature of metabolism (Postgate, 1984). A variety of electron donors such as lactate or pyruvate may be utilized in the anaerobic respiration of sulfate (Widdel, 1988). An unmistakable end product of sulfate reduction is the odiferous hydrogen sulfide gas. This reduction process is dissimilatory because it occurs for bioenergetic purposes, as opposed to the assimilatory sulfate process, in which the reduced sulfur is incorporated into biological molecules (Kredich, 1996).

The generation of hydrogen sulfide by the sulfate reducing bacteria poses significant economic concerns because of the corrosive nature of sulfide on ferrous metals and concrete. One example is the corrosion of concrete conduits of sewage systems. This occurs as a consequence of the interaction of sulfate-reducing and sulfide-oxidizing metabolic processes (Odom, 1993). In biofilm communities at the bottom of sewer pipes, where oxygen has been depleted by organic catabolism, SRB generate copious hydrogen sulfide. In the oxygenic environment in the condensate at the top of the pipes, aerobic sulfide-oxidizing organisms generate sulfuric acid that corrodes the concrete. In regions such as Phoenix and Denver, where the sewage system is very flat, this type of damage is prevalent, as sewage drainage is never complete and high summertime temperatures are conducive to rapid microbial growth.

In addition to concrete corrosion, the generation of hydrogen sulfide can result in corrosion of metals, especially ferrous metals, leading to the destruction of wells and pipelines (Hamilton, 1985). The cathodic depolarization mechanism of anaerobic iron biocorrosion proposed in 1934, by Von Wolzogen Kühr and Van der Vulgt, likely contributes to this phenomenon (Von Wolzogen Kuhr and van der Vulgt, 1934). Cathodic depolarization may occur when the surface of the metal becomes depolarized and cathodic and anodic reactions occur due to the interaction of bacteria with the metal (Figure 1.1). Electrons from the metal reduce protons from the water to atomic hydrogen, where SRB remove it by oxidation. Metal ions are solubilized and corrosion occurs.

Figure 1.1. Mechanism of cathodic depolarization of iron (Von Wolzogen Kuhr and van der Vulgt, 1934) and corrosion of metal pipes. (Corroded iron pipe picture from U.S. Department of Labor, Occupational Health and Safety Administration website, http://www.osha.gov.)

Sulfate reducing
bacteria
S^{2-}
SO_4^{2-}
$4\ H_2O$
$4\ H_2$
$8\ H^+$
$3\ Fe^{2+}$
$4\ Fe^{2+}$
FeS
ferrous metal
Cathode
aqueous environment
$8\ e^-$
Anode
Fe^0

Another deleterious effect of SRB occurs in the oil industry. The generation of hydrogen sulfide causes oil well souring due to increased content of dissolved sulfide in the oil and iron sulfide precipitates that plug oil well pipes and machinery (Odom, 1993). The result is sulfur-contaminated petroleum products, which contribute to pollution and necessitate great efforts to clean. An even greater problem is the loss of human life resulting from inhalation of poisonous hydrogen sulfide gas when oil well workers enter contaminated well areas or trapped gas under offshore oil platforms. OSHA warns that levels of 300 ppm cause the olfactory nerve to lose sensitivity. The "rotten egg" odor that is noticeable in the first few breaths is no longer detectable. At levels of 600 ppm the gas has filled the lungs and breathing becomes difficult. At higher levels, paralysis of the lungs occurs, resulting in death (U.S. Department of Labor, Occupational Health and Safety Administration website, http://www.osha.gov).

II. Bioremediation Potential

Nuclear waste in the environment is an enormous problem. The U.S. Department of Energy has compiled alarming statistics regarding nuclear waste, including the existence of 7,000 structures in 120 sites in 36 states (Program, 2003). Additionally, there are about 1.7 trillion gallons of contaminated ground water and 40 million cubic meters of contaminated soil. Many of these contaminated sites came about from nuclear weapons production reactors operational during the Cold War and are no longer in use today. According to U.S. Department of Energy statistics published in 2003, the clean up costs for current projects total $220 billion and expected completion is greater than 70 years. This cost could rise beyond $300 billion dollars unless more efficient clean-up strategies are devised (Program, 2003).

Bioremediation, the use of microorganisms to eliminate, contain, or transform environmental contaminants, has been utilized to treat solvent and explosive containants effectively (Program, 2003), and it holds promise for toxic metals and metalloids. Two of the most common hazardous materials are radionuclides, such as uranium and technetium, and toxic metals, such as chromium, arsenic, and mercury. The ability of sulfate reducing bacteria to respire metals may provide an effective and efficient means of bioremediation. The addition of electrons to the metals results in an alteration of the redox state that changes the solubility of a number of radionuclides and metals. Of particular environmental interest is the enzymatic reduction of uranium from soluble U(VI) to the insoluble mineral uraninite U(IV) (Lovley, 1993). Although the radioactivity of the metal is unaffected, the change in solubility would provide a way to filter and collect uranium contaminants from groundwater. It has been found *in situ* in contaminated water and soil that the reduction of uranium(VI) and technetium(VII) by SRB can be stimulated by the addition of nutrients such as lactate into the environment (Abdelouas, 2000; 2002).

There are a number of advantages to utilizing SRB for bioremediation. First, these bacteria naturally reside in the soil and water microbial community (Abdelouas, 2000). Second, current remediation methods, such as excavation and subsequent treatment of contaminated soil and water, are extremely destructive to the environment. In contrast, it is envisioned that the use of bacteria already present the in the environment would pose considerably less impact (Program, 2003). A complete understanding of the mechanisms involved in the reduction of metals would enable more effective utilization of the SRB in bioremediation.

III. Properties of *Desulfovibrio desulfuricans* G20

Desulfovibrio desulfuricans G20 was the sulfate-reducer chosen for use in this study (Figure 1.2). This Gram-negative bacterium is strictly anaerobic and was originally isolated from an oil well corrosion site (Weimer, 1988). It was selected for spontaneous nalidixic acid resistance and cured of the cryptic endogenous plasmid pBG1 (Wall, 1993). This bacterium is easily cultivated in defined media in an anaerobic chamber and is genetically accessible, as it is transformable by standard techniques such as electroporation (Rousset, 1998) and it participates in conjugation (Argyle, 1992; Van den Berg, 1989) Various antibiotic sensitivities are available for such genetic manipulations of SRB. The genome sequence of *D. desulfuricans* G20 has been completed by the U.S. Department of Energy at the Joint Genome Institute by Paul Richardson and is currently available for research (genome annotation found at The Virtual Institute for Microbial Stress and Survival, VIMSS, http://www.escalante.lbl.gov).

Figure 1.2. Scanning electron micrograph of *Desulfovibrio desulfuricans* G20. Prepared by Barbara Giles and University of Missouri Electron Microscopy Core Facilities.

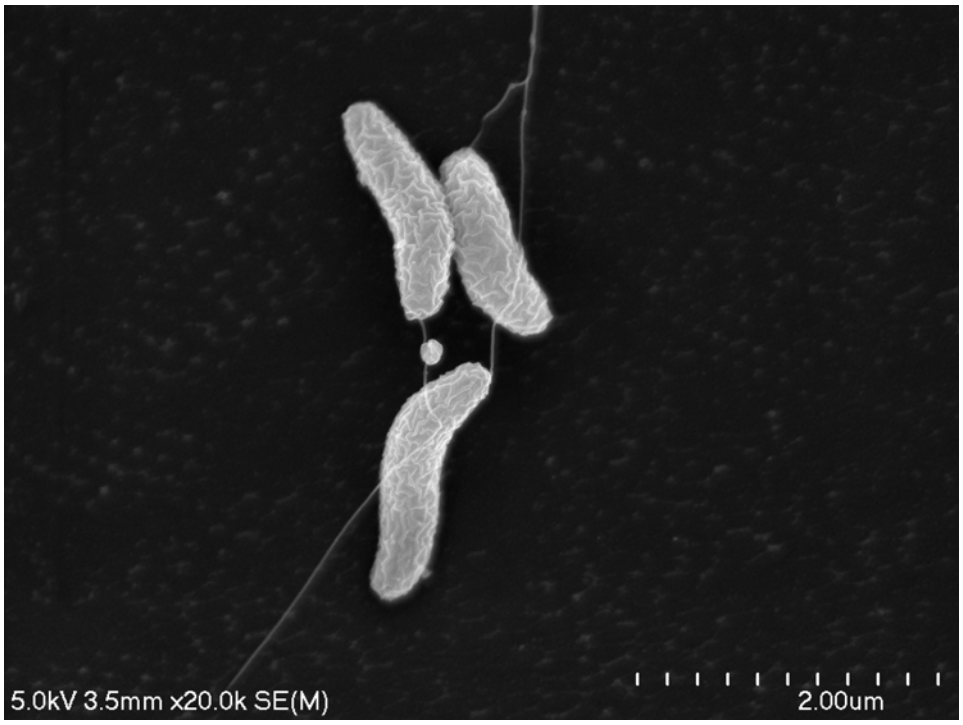
5.0kV 3.5mm x20.0k SE(M)
2.00um

IV. Bioenergetic Pathway

In order to utilize SRB for bioremediation, a more complete understanding of the bioenergetic pathway is necessary (Figure 1.3). It is known that *Desulfovibrio* can be cultivated with hydrogen gas as a sole electron donor (Postgate, 1984). It has been hypothesized that hydrogen is oxidized by the Fe-hydrogenase in the periplasm (Pohorelic, 2002) and in turn electrons are transferred to the periplasmic cytochrome c_3. It is proposed that the electrons pass through a transmembrane complex into the cytoplasm where the terminal electron acceptor, sulfate, is reduced to sulfide. The periplasmic electron transport chain is likely to be a complex network of electron carrier proteins and it has been observed in *Desulfovibrio* that mutations in individual electron carriers can be compensated (Dolla et al. 2000; Pohorelic, 2002; Rapp-Giles, 2000).

Protons generated are available to form a proton gradient that supports the production of ATP through the membrane-bound ATPase. The formation of the proton gradient across the cytoplasmic membrane, as proposed by Mitchell *et al.* (1965), suggests that as electrons reduce a terminal electron acceptor, such as sulfate, a separation of charge takes place such that a positive charge exists in the periplasm, creating an energy gradient which drives ATP synthesis through ATPase. Alternatively, hydrogen cycling proposed by Odom *et al.* (1981) suggests that as cytoplasmic hydrogenases catalyze the heterolytic cleavage of hydrogen, H_2 gas is permitted to diffuse across the cell membrane where it is recaptured by periplasmic hydrogenases. Noguera *et al.* (1998) used mathematical modeling and growth culture experiments in *Desulfovibrio vulgaris* to discover that both electron transport and hydrogen cycling are used to establish a gradient.

Figure 1.3. Model for the bioenergetic pathway for SRB. In this model hydrogen is oxidized by the hydrogenases in the periplasm and electrons are transferred to the periplasmic cytochrome c_3. Electrons are then passed through a transmembrane complex into the cytoplasm where the terminal electron acceptor, sulfate, is reduced to sulfide. Protons form a proton gradient that supports the production of ATP through the membrane-bound ATPase. Figure adapted from (Heidelberg, 2004).

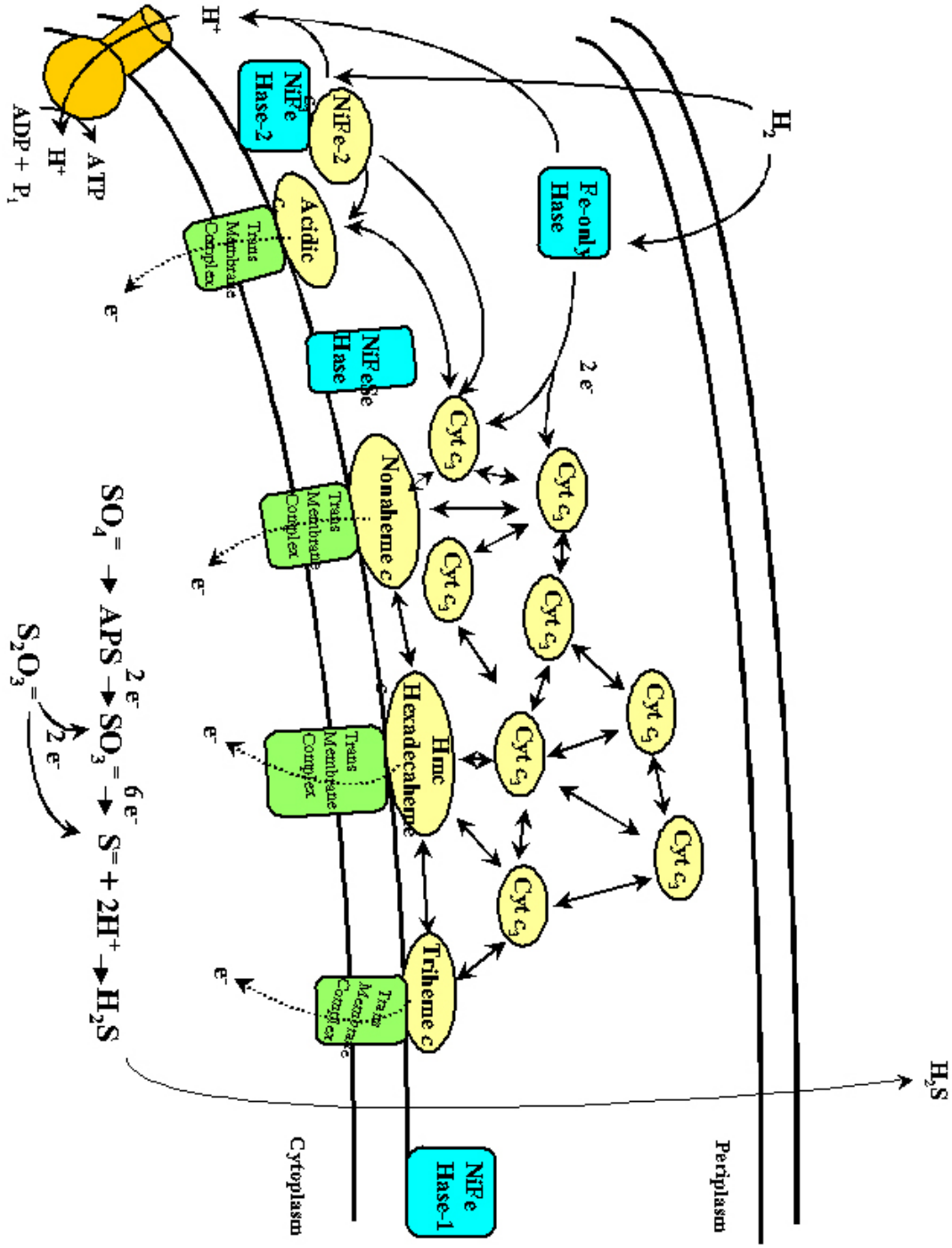
H2
Fe-only Hase
NiFe-2
NiFe Hase-2
Acidic c
NiFe Hase
Nonaheme c
Hmc Hexadecaheme c
Triheme c
NiFe Hase-1
Trans Membrane Complex
Cyt c3
2 e-
H+
ATP
ADP + Pi
e-
SO4= → APS → SO3= → S= + 2H+ → H2S
S2O3=
2 e-
6 e-
Periplasm
Cytoplasm
H2S

V. Cytochrome c_3

The electrons generated in the cytoplasm of *Desulfovibrio* during respiration are transported through a network of electron carrier proteins including cytochromes (Figure 1.3). The tetraheme cytochrome c_3 (*M*r 13,000) is the most abundant *c*-type cytochrome found in the periplasm of many species of SRB, encompassing 80% of the cytochromes in the periplasm of *Desulfovibrio vulgaris* (Aubert, 1998), and was proposed to be involved in the reduction of uranium in a model tested *in vitro* by Lovley *et al.* (1993). It was found that when the soluble cell fraction of *D. vulgaris* was passed over a cationic column to remove cytochrome c_3, U(VI) reduction did not occur. However, reduction of U(VI) was restored when purified cytochrome c_3 was added back to the soluble fraction. In this model electrons are shuttled through cytochrome c_3 where U(VI) is reduced to U(IV) by the gain of two electrons.

To examine this model *in vivo* a cytochrome c_3 mutant was constructed by the plasmid interruption of the monocistronic chromosomal copy of the *cycA* gene (Rapp-Giles, 2000). The reduction of uranium in the wild-type and the *cycA* mutant was assayed enzymatically *in vitro* by measuring the concentration of U(VI) in solution with a kinetic phosphorescence analyzer over the course of 25 hours (Payne, 2002). In the cytochrome c_3 mutant the rate of U(VI) removal was decreased by about half that of wild-type when lactate was used as an electron donor, and was decreased by about 33% that of wild-type when pyruvate was used as an electron donor. When hydrogen was used as an electron donor, the rate of U(VI) reduction was impaired to about 10% that of wild-type (Figure 1.4) (Payne, 2002). These experiments provided evidence that cytochrome c_3 is involved

in electron flow to U(VI), although in its absence alternative electron carriers may be utilized.

Figure 1.4. U(VI) reduction by wild-type and *cycA*$^-$ mutant (Payne, 2002). Ten millimolar sodium lactate (0), 10 mM sodium pyruvate (Δ), 1 atm hydrogen gas (□), or no electron donor (◊) was added to samples containing 1mM uranyl acetate and 200 μg of whole-cell protein/ml and the concentration of U(VI) was measured over a time course of 25 hours. Whole cell assays contained 1mM uranyl acetate in anaerobic sodium bicarbonate buffer. Growth and manipulations were carried out in the anaerobic chamber at 31°C. The disappearance of U(VI) from solution was monitored with a phosphorescence analyzer.

Wild type

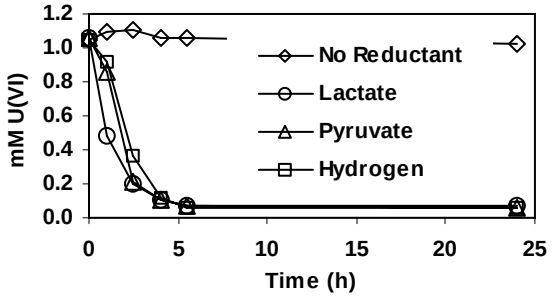

CycA-

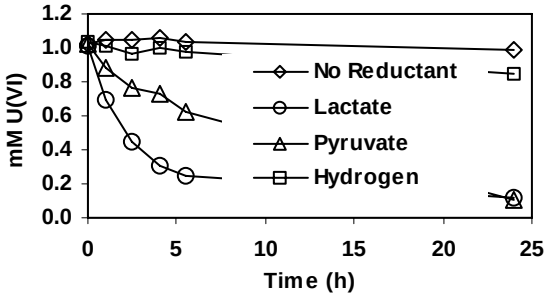

In this investigation amino acid residues chosen to be candidates for site directed mutagenesis were identified by protein alignments comparing cytochromes from different species and targeting conserved residues (Figure 1.5). Phenylalanine 20 (*D. vulgaris* Hildenborough numbering) is a conserved residue shown to be significant in electron transfer. In *D. vulgaris* Hildenborough, phenylalanine 20 has been suggested to be involved in the electron flow within the cytochrome (Dolla, 1991). In earlier work, this residue was replaced with the nonaromatic hydrophobic residue leucine and electron transfer properties were examined by measuring the kinetics of reduction of the mutant cytochrome by the Fe-hydrogenase (Dolla, 1991). The F20L mutant was impaired in intermolecular cooperativity compared to wild-type. Also, in *Desulfovibrio vulgaris* Miyazaki cytochrome c_3, decreases in redox potential of heme groups were observed in F20 mutants (Takayama, 2004). To investigate the importance of the corresponding residue in *D. desulfuricans* G20 cytochrome c_3, phenylalanine 19 (*D. desulfuricans* G20 numbering) was replaced with the nonaromatic residue alanine (Figure 1.6).

A list of critical amino acid residues of cytochrome c_3 that have been investigated by site-specific mutation in other *Desulfovibrio* species is presented in Table 1.1. One residue, tyrosine 27 in the vicinity of heme 1 was chosen for analysis because of the importance of aromatic amino acids in other investigations. Ozawa *et al.* (2003) investigated the structural and redox properties of tyrosine 43 mutants of cytochrome c_3 of *D. vulgaris* Miyazaki. In kinetic experiments, significant differences were observed in the rate of reduction as a result of replacing this aromatic residue with a neutral non-aromatic residue (Ozawa, 2003). In this study, tyrosine 27 was replaced with alanine (Figure 1.6).

Figure 1.5. Amino acid sequence alignments of type 1 tetraheme cytochrome c_3 molecules of *Desulfovibrio*, cytochrome c_3 of *D. vulgaris* strain Hildenborough (DvH) (NCBI accession # P00131), *D. vulgaris* strain Miyazaki (DvM) (NCBI accession # P00132), *D. desulfuricans* strain G20 (DdG20) (NCBI accession # AAF17604), *D. gigas* (DGigas) (NCBI accession # P00133), and *D. desulfuricans* strain Norway (DdN) (NCBI accession # P00136). Green squares highlight each of the heme binding sites and red squares indicate residues chosen for mutation in this study. Blue lines indicate site of cleavage of signal sequence.


Heme 1
DvH MRK-LFFCGVLALAVAFALP-VVAAPKAPADGLKMEATKQPVVFNHSTHKSVKCGDCHHP
DvM MKK-MFLTGVLALAVAIAMPALAAAPKAPADGLKMDKTKQPVVFNHSTHKAVKCGDCHHP
DdG20 MRKSLFAVMVLALVAAFALP--VIAAEAPADGLKMENTKMPVIFNHSSHSSYQCADCHHP
DGigas ----------VDVP----ADGAKIDFIAGGEKNLTVVFNHSTHKDVKCDDCHHD
DdN ---------ADAPGDDYVIS-APEGMKAKPKGDKPGALQKTVPFPHTKHATVKCVQCHHT
Heme 2
Heme 3
DvH VNGKEDY-RKCGTAGCHDSMDKKDKSAKGYYHVMHD-KNTKFKSCVGCHVEVAGADAAKK
DvM VNGKEDY-QKCATAGCHDNMDKKDKSAKGYYHAMHD-KGTKFKSCVGCHLETAGADAAKK
DdG20 VNGKENL-AKCATAGCHDVFDKKDKSVHSYYKIIHDRKATTVATCMSCHLEAAGSDKDLK
DGigas P-GDKQY-AGCTTDGCHNILDKADKSVNSWYKVVHDAKGGAKPTCISCHKDKAGDDKELK
DdN LEADGGAVKKCTTSGCHDSLEFRDKANAKD---IKLVESAFHTQCIDCHALKKKDKKPTG
Heme 4
DvH KDLTGCKKSKCHE--
DvM KELTGCKGSKCHS--
DdG20 KELTGCKKSKCHP--
DGigas KKLTGCKGSACHPS-
DdN P--TACG--KCHTTN

Figure 1.6. Cytochrome c_3 structure (Pattarkine et al., in preparation) highlighting mutated residues including F19A, Y27A, and C45A.

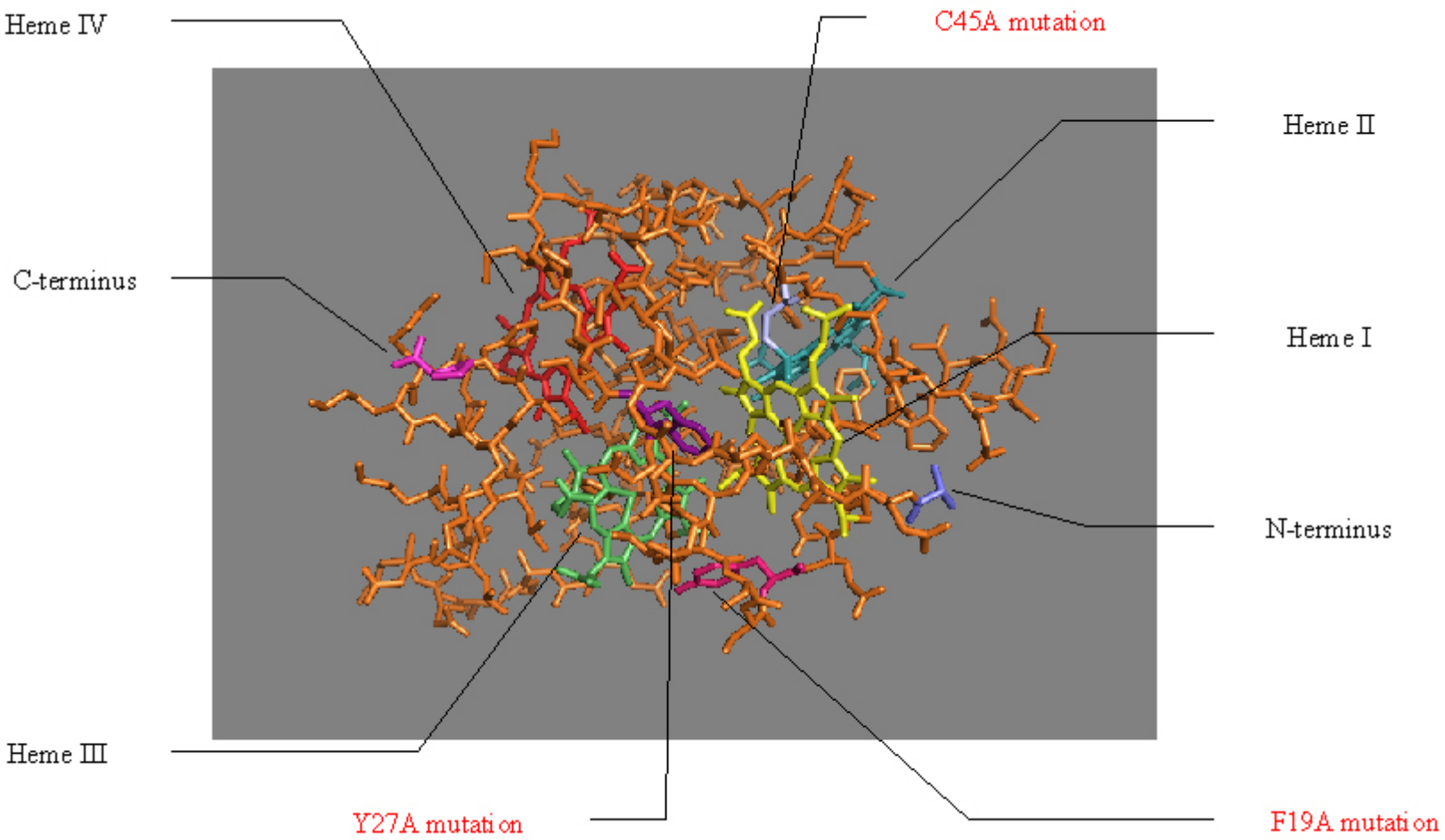
Heme IV
C45A mutation
Heme II
C-terminus
Heme I
N-terminus
Heme III
Y27A mutation
F19A mutation

Table 1.1. Site-specific amino acid mutations of cytochromes c_3 reported in recent literature. Amino acid residues mutated, results, methods, and references are shown.

Title	Roles of Noncoordinated Aromatic Residues in Redox Regulation of Cytochrome c_3 from *Desulfovibrio vulgaris* Miyazaki F
Organism/cytochrome	*Desulfovibrio vulgaris* Miyazaki F, cytochrome c_3
Mutations	F20A, F20E, F20M, F20H, F20Y, Y65A, Y65F, Y65L, Y66F, Y66L, H67A, H67F, H67Q, F76L, F76Y, and double mutation Y43L/Y66L
Objective	Systematic analysis of aromatic residues to determine the role of aromatic residues in the reduction of redox potential
Result	The mutations at Phe20 induced large chemical shift changes in the NMR signals for hemes I and 3, and large changes in the microscopic redox potentials of hemes I and 3.
Crystal Structures	F20L (earlier article)
Methods	Mutated genes were expressed in *Shewanella oneidensis* TSP-C, differential pulse polarography, and NMR
Reference	Takayama, 2004

Title	Role of the aromatic ring of Tyr43 in tetraheme cytochrome c3 from *Desulfovibrio vulgaris* Miyazaki F
Organism/cytochrome	*Desulfovibrio vulgaris* Miyazaki F, cytochrome c_3
Mutations	Y43L, Y43F
Objective	To investigate the structural and redox properties, and electron transfer kinetics of two mutations
Result	The replacement of tyrosine with leucine increased the redox potential of heme 1 by 44 and 35 mV at the first and last reduction steps, respectively; its effects on the other hemes are small. Temperature-dependent line-width broadening in partially reduced samples established that the aromatic ring at position 43 participates in the control of the kinetics of intramolecular electron transfer.
Crystal Structures	Y43L
Methods	Mutated genes were expressed in *Shewanella oneidensis* TSP-C, NMR, laser flash photolysis, and crystallization
Reference	Ozawa, 2003

Title	Effect of hydrogen-bond networks in controlling reduction potentials in *Desulfovibrio vulgaris* (Hildenborough) cytochrome c_3 probed by site-specific mutagenesis
Organism/cytochrome	*Desulfovibrio vulgaris* Hildenborough, cytochrome c_3
Mutations	T24L
Objective	To investigate the effect of redox-linked conformational change observed at residue T24 on the general redox properties, T24L mutation created and thermodynamic properties examined
Result	The NMR spectra of the mutated protein are very similar to

	those of the wild type, showing that the general folding and heme core architecture are not affected by the mutation. However, thermodynamic analysis of the mutated cytochrome reveals a large alteration in the microscopic reduction potential of heme III.
Crystal Structures	no
Methods	Mutated cytochrome was produced in *Desulfovibrio desulfuricans* G200, visible redox titration, NMR, computer modeling
Reference	Salgueiro, 2001

Title	Key role of phenylalanine 20 in cytochrome c_3: Structure, stability, and function studies
Organism/cytochrome	*Desulfovibrio vulgaris* Hildenborough, cytochrome c_3
Mutations	F20L
Objective	To determine the role of Phe20 in folding and electron transferring properties
Result	The F20L replacement did not have any strong effects on the heme region stability, a decrease of the thermostability of the whole molecule was observed. The F20L replacement itself and/or this structural modification might be responsible for the loss of the intermolecular cooperativity between F20L cytochrome c_3 molecules.
Crystal Structures	F20L
Methods	Mutated cytochrome was produced in *Desulfovibrio desulfuricans* G200, isoelectric point measurement, mass spectrometry, plasma emission spectrometry, amino acid sequencing, scanning microcalorimetry, circular dichroism, and crystallization
Reference	Dolla, 1999

Title	Replacement of lysine 45 by uncharged residues modulates the redox-Bohr effect in tetraheme cytochrome c_3 of *Desulfovibrio vulgaris* (Hildenborough)
Organism/cytochrome	*Desulfovibrio vulgaris* Hildenborough, cytochrome c_3
Mutations	K45T, K45Q, K45L
Objective	To investigate the structural basis for pH dependence of the redox potential by mutation of Lys45, a charged residue in the vicinity of heme I
Result	The analysis of the redox interactions as well as the redox-Bohr behavior of the mutated cytochromes c3 allowed the conclusion that residue 45 has a functional role in the control of the pKa of the propionate groups of heme I and confirms the involvement of this residue in the redox-Bohr effect.

Crystal Structures	no
Methods	Mutated cytochrome was produced in *Desulfovibrio desulfuricans* G200, UV spectroscopy, redox titrations, and NMR
Reference	Saraiva, 1998

Title	Structural and kinetic studies of the Y73E mutant of octaheme cytochrome c_3 (Mr = 26 000) from *Desulfovibrio desulfuricans* Norway
Organism/cytochrome	*Desulfovibrio desulfuricans* Norway, octaheme cytochrome c_3
Mutations	Y73E
Objective	To utilize structural, kinetic, and interaction studies to investigate the role of the highly conserved aromatic residue, Tyr73, parallel to the sixth heme axial ligand of heme 4
Result	The kinetic experiments show that the Y73E replacement provokes no significant change in the electron-transfer reaction with the physiological partner, the [NiFeSe] hydrogenase, but that the protein-protein interaction between cytochrome c3 (Mr = 26 000) and hydrogenase is strongly affected by the mutation.
Crystal Structures	Y73E
Methods	Mutated cytochrome was produced in *Desulfovibrio desulfuricans* G201, BIAcore, kinetic experiments, and crystallization
Reference	Aubert, 1998

Title	A single mutation in the heme 4 environment of *Desulfovibrio desulfuricans* Norway cytochrome c_3 (m-r 26,000) greatly affects the molecule reactivity
Organism/cytochrome	*Desulfovibrio desulfuricans* Norway, octaheme cytochrome c_3
Mutations	Y73E
Objective	To study the physiochemical properties of *Desulfovibrio desulfuricans* Norway cytochrome c_3 (m-r 26,000) and the importance of highly conserved residues
Result	A global increase of the oxidoreduction potentials of about 50 mV is measured for the Y73E cytochrome. The mutation also has a strong influence on the interaction of the cytochrome with its redox partner, the hydrogenase. This suggests, like the tetraheme cytochrome c(3) (M-r 13,000), heme 4 is the interactive heme in the cytochrome-hydrogenase complex and that alteration of the heme 4 environment can greatly affect the electron transfer reaction with its redox partner.
Crystal Structures	no
Methods	Mutated cytochrome was produced in *Desulfovibrio desulfuricans* G201, BIAcore, protein sequencing, determination

	of oxidoreduction potential, and isoelectric point determination
Reference	Aubert, 1997

Title	Evaluation of the role of specific acidic amino acid residues in electron transfer between the flavodoxin and cytochrome c_3 from *Desulfovibrio vulgaris*
Authors	Feng and Swensen
Organism/cytochrome	*Desulfovibrio desulfuricans* Hildenborough, flavodoxin
Mutations	D69N, D70N, D127N, D129N
Objective	To investigate the ability of mutant proteins to accept electrons from cytochrome c_3
Result	A minimal electron transfer mechanism is proposed in which an initial complex is formed that is stabilized by intermolecular electrostatic interactions but is relatively inefficient in terms of electron transfer. This step is followed by a rate-limiting reorganization of that complex leading to efficient electron transfer. The apparent rate of this reorganization step was enhanced by the disruption of the initial electrostatic interactions through the neutralization of certain acidic amino acid residues leading to faster overall observed electron transfer rates at low ionic strengths.
Crystal Structures	no
Methods	Mutated protein was produced in *E. coli* and purified on hydroxyl appetite column, spectroscopic measurements, and kinetic measurements
Reference	Feng, 1997

Title	Drastic influence of a single heme axial ligand replacement on the thermostability of cytochrome c_3
Organism/cytochrome	*Desulfovibrio vulgaris* Hildenborough, cytochrome c_3
Mutations	H22M, H25M, H35M, H70M
Objective	To study the thermostability of wild type *Desulfovibrio vulgaris* is Hildenborough tetraheme cytochrome c_3 and its H22M, H25M, H35M and H70M mutants
Result	Mutations do not change overall secondary structure and local structure of the hemes vicinity. All mutants are much more unstable to heat denaturation than the wild type cytochrome. The heme region is important not only for the functional properties of the cytochrome but also for the overall protein thermostability.
Crystal Structures	no
Methods	Mutated cytochrome was produced in *Desulfovibrio desulfuricans* G200, circular dichroism
Reference	Dolla, 1995

Title	Electrostatic effects of surface acidic amino acid residues on the oxidation-reduction potentials of the flavodoxin from *Desulfovibrio vulgaris* (Hildenborough)
Organism/cytochrome	*Desulfovibrio vulgaris* flavodoxin
Mutations	D62N, D63N, E66Q, D95N, E99Q, D106N, D62N/D63N, D62N/E66Q, D63N/E66Q, D95N/E99Q, D95N/D106N, E99Q/D106N, D62N/D63N/E66Q, D95N/E99Q/D106N, D62N/D63N/E66Q/E99Q, D62N/D63N/E66Q/E99Q/D106N,D62N/D63N/E66Q/D95N/ E99Q/D106N
Objective	To investigate the contributions of six acidic residues-Asp62, Asp63, Glu66, Asp95, Glu66, Asp95, Glu99, and Asp106-in establishing the redox properties of the FMN cofactor in the *D. vulgaris* flavodoxin
Result	There was no obvious correlation between the midpoint potentials for the oxidized/semiquinone couple and general electrostatic environment, although some differences were noted. However, the midpoint potential for the semiquinone/hydroquinone couple for each of the mutants was less negative than that of the wild type. These increases are strongly correlated with the number of acid to amide substitutions.
Crystal Structures	no
Methods	Mutated flavodoxin was produced in *E. coli*, mid-point determination
Reference	Zhou, 1995

Title	Characterization and oxidoreduction properties of cytochrome after heme axial ligand replacements c_3
Organism/cytochrome	*Desulfovibrio vulgaris* Hildenborough, cytochrome c_3
Mutations	H22M, H25M, H35M, H70M
Objective	To perform biochemical and electrochemical characterizations of various mutants in which the sixth acial ligand of each heme has been replaced by methionine
Result	The novel methionine was correctly coordinated to the iron atom of hemes 3 and 4 in H25M and H70M cytochromes c_3, respectively, and this coordination induced a large increase in the oxidoreduction potential of the mutated heme. In contrast, in the case of H22M and H35M cytochromes c_3, in which the corresponding methionine is in an oxidized form, only slight changes in redox potential values were observed.
Crystal Structures	no
Methods	Mutated cytochrome was produced in *Desulfovibrio desulfuricans* G200, protein sequencing, mass spectrometry, UV spectrometry, and electrochemistry

Reference	Dolla, 1994

Title	Site-directed mutagenesis of tetraheme cytochrome c_3 Modification of oxidoreduction potentials after heme axial ligand replacement
Organism/cytochrome	*Desulfovibrio vulgaris* Hildenborough, cytochrome c_3
Mutations	H70M
Objective	To complete the assignment of the heme redox potentials and elucidate their function by establishing the effect of replacement of His70
Result	A large increase of at least 200 mV of one of the four oxidation-reduction potentials was observed by electrochemistry and is interpreted in terms of structure/potential relationships.
Crystal Structures	no
Methods	Mutated cytochrome was produced in *Desulfovibrio desulfuricans* G200, UV spectroscopy, NMR, computer modeling, electrochemistry
Reference	Mus-Veteau, 1992

Lastly, the cytochrome c_7 of *Desulfuromonas acetoxidans* contains only three hemes and is able to function as an electron transfer protein in sulfur metabolism (Pereira, 1997). The crystal structure of cytochrome c_7 is available (Assfalg, 2002) and is similar to cytochrome c_3 except for the absence of heme 2 (Figure 1.7). To imitate cytochrome c_7 and test electron transfer functionality, heme 2 was disrupted by the replacement of cysteine 45 with alanine (Figure 1.6).

A second set of targets for site-specific mutation were chosen as amino acid residues projected to be a point of interaction between cytochrome c_3 and molybdate. The cytochrome c_3 protein was purified and crystallized (Pattarkine *et al.*, in preparation). From those crystals, the structure of cytochrome c_3 was determined at 1.5 Å resolution. The crystal structure has enabled identification of a second set of amino acid residues that are potentially critical for interaction with molybdate. In the unpublished results of Pattarkine *et al.*, the crystal structure of the oxidized cytochrome c_3 protein bound to the molybdate ion identified the site of interaction between the cytochrome and the metal near heme 4 (Figure 1.8). In this study four amino acid residues were mutated and the ability of one of the mutant proteins to transfer electrons to molybdate or uranium was examined (Figure1.9).

Figure 1.7. *Desulfuromonas acetoxidans* cytochrome c_7 structure (Assfalg, 2002), and *Desulfovibrio desulfuricans* G20 cytochrome c_3 structure (Pattarkine et al., in preparation).

Desulfovibrio acetoxidans cytochrome c_7

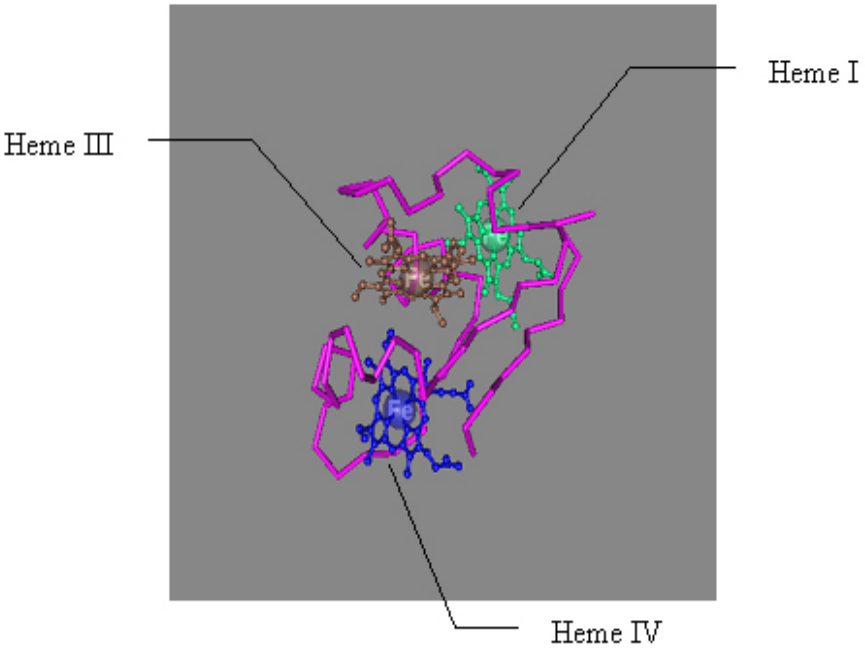

Desulfovibrio desulfuricans G20 cytochrome c_3

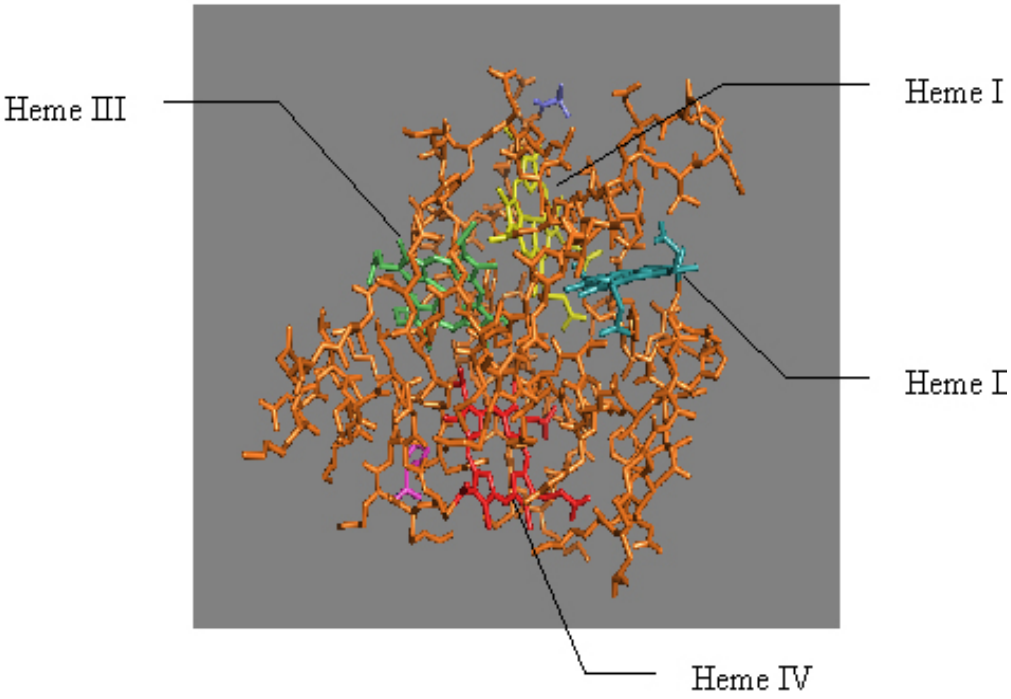

Figure 1.8. *Desulfovibrio desulfuricans* G20 cytochrome c_3 crystal structure with molybdate (Pattarkine, *et al.*, manuscript in preparation). The oxidized, reduced, and molybdate-bound forms of *D. desulfuricans* c_3 are colored green, red and yellow, respectively. The structure of *D. vulgaris* Hildenborough c_3 is shown in blue. The hemes are labeled with Roman numerals. The molybdate ion is present in the vicinity of heme 4.

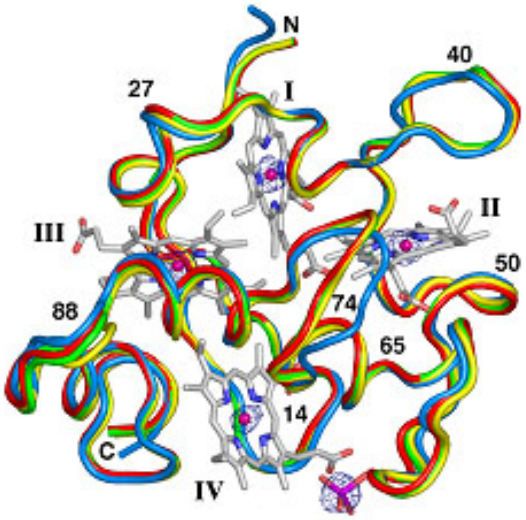
N
40
27
I
II
III
50
88
74
65
14
C
IV

Figure 1.9. Cytochrome c_3 structure (Pattarkine et al., in preparation) highlighting mutated residues including K14A, K66A, K72A, and M80K.

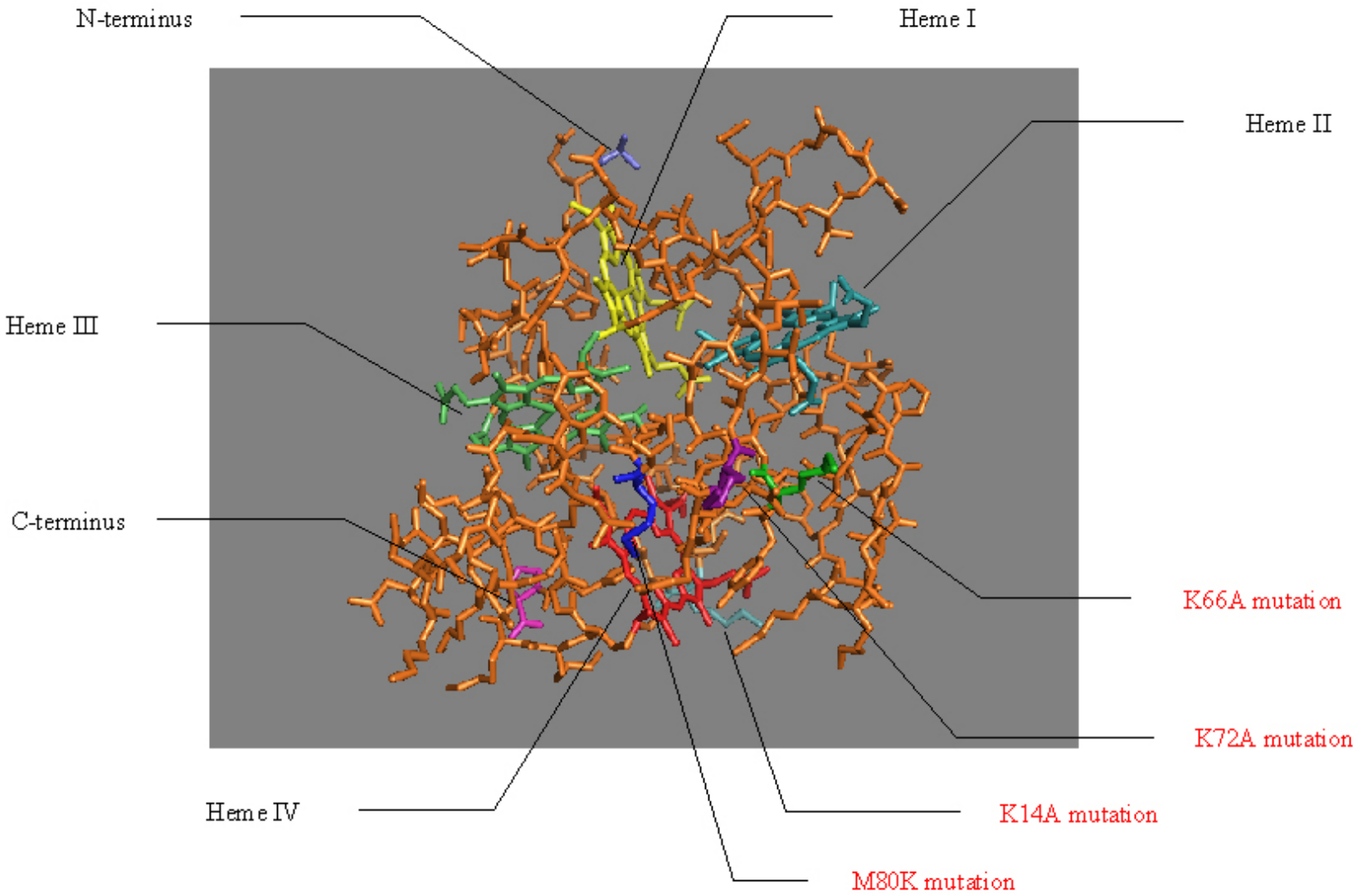
N-terminus
Heme I
Heme II
Heme III
C-terminus
K66A mutation
K72A mutation
Heme IV
K14A mutation
M80K mutation

VI. Cytochrome c_3 Maturation

Specific residues of the cytochrome c_3 protein were mutated and the electron transfer capabilities of the mutant proteins were tested. In order to purify wild-type and mutant cytochromes, a suitable protein expression system was required. A system was developed to enable expression of cytochrome proteins in *E. coli* by expressing cytochrome maturation genes with the cytochrome gene of interest (Arslan, 1998).

Cytochrome maturation involves the structural rearrangement of the linear polypeptide, or apocytochrome, into the folded protein containing covalently bound heme groups. In *E. coli* it has been shown that cytochrome *c* maturation genes, *ccmABCDEFGH*, are essential for this process in addition to several genes of the general secretory pathway and cellular redox control genes. Functions of the Ccm proteins include an ABC transporter, heme delivery system, and redox-control system. The sequence of steps involved is as follows:

1. The N-terminal sequence directs the precursor protein from its place of synthesis, in the cytoplasm, to its place of function, which is in the periplasm. Once in the periplasm the N-terminal sequence is cleaved. Precursors are translocated to periplasm by the type II secretion pathway before ligation of heme occurs (Thony-Meyer, 1997). Heme must also be translocated from the cytoplasm; however, the mechanism is yet to be determined. It has been hypothesized that an ABC transporter may translocate heme to the periplasm (Schulz, 1999).
2. Apocytochromes are prepared for heme binding by reduction of cysteine residues in the CXXCH motif.

3. The last step in the maturation process is the specific insertion of heme into the polypeptide. A periplasmic heme binding chaperone is proposed to be involved in the correct placement and covalent incorporation of the heme (Schulz, 2000; Thony-Meyer, 2003).

A summary of the genes involved in these processes and hypothetical function of gene products is given on Table 1.2.

Previously, cytochrome overproduction in *E. coli* was limited by the expression of genes required for cytochrome maturation. Thony-Meyer *et al.* (2003) cloned *E. coli ccmABCDEFGH* genes into the plasmid, pEC86, from which the genes are constitutively expressed. Plasmid pEC86 was then co-transformed with a plasmid containing the cytochrome gene to be expressed. This was found to increase expression of both endogenous and foreign cytochromes (Arslan, 1998). This has proven to be an effective tool enabling high efficiency synthesis of cytochrome molecules from various species (Londer, 2002; Da Costa, 2000).

Table 1.2. Cytochrome maturation genes and functions. Table generated based on information published in a review by Thony-Meyer (2002).

Gene	Function of gene product	References
ccmA	subunit of ABC transporter, peripheral membrane protein with well conserved ATP binding cassette, associates with CcmB	(Goldman, 1997a; Goldman, 1997b)
ccmB	subunit of ABC transporter, integral membrane protein that spans lipid bilayer, believed to be permease for an unidentified substrate	(Goldman,1997a; Goldman, 1997b; Schulz, 1999; Page, 1997)
ccmC	possibly a member of ABC transporter, function is not resolved, protein has unique involvement in heme transfer to CcmE, and therefore a function independent of CcmAB	(Goldman,1997a; Goldman, 1997b; Page, 1997; Schulz, 1999)
ccmD	small membrane protein with a highly charged C-terminal domain in the cytoplasm, stabilizes CcmE in the membrane and is involved in interaction between CcmC and CcmE	(Thony-Meyer, 2002; Schulz, 1999; Schulz, 2000)
ccmE	periplasmic heme chaperone, binds heme transiently and is believed to be an intermediate in heme delivery system, heme transport across the membrane occurs before binding to CcmE and CcmC is necessary for binding to CcmE	(Schulz, 1998; Reid, 1998; Deshmukh, 2000; Schulz, 2000; Spielewoy, 2001)
ccmF	required for the transfer of heme from CcmE to cytochrome c, shown to interact with CcmE and CcmH	(Schulz, 1999; Ren, 2002; Thony-Meyer, 2002)
ccmG	periplasmic thioredoxin, interacts with periplasmic domain of DsbD, electron transfer to CcmG and CcmH occurs via DsbD	(Fabianek, 2000; Reid, 2001; Fabianek, 1998; Katzen, 2000)
ccmH	hypothesized role is recognition of heme binding sites in the apocytochrome, and interact with binding sites providing guidance for the CcmE-CcmF complex in order for heme attachment to take place	(Ren, 2001; Thony-Meyer, 1997; Thony-Meyer, 2000; Reid, 2001)
DsbD	transmembrane protein, periplasmic domain interacts with CcmG, transfers electrons from cytoplasm to periplasm	(Katzen, 2000; Thony-Meyer, 2002)

VII. Specific Aims

The predominant tetraheme c-type cytochrome c_3 of *D. desulfuricans* plays a critical role in the reduction of U(VI) to U(IV) either directly or indirectly (Payne, 2002). The purpose of this investigation was to mutate specific conserved amino acid residues, a first set chosen based on the available literature, and a second set based on the hypothetical site of interaction between cytochrome c_3 and metals. The wild-type and mutant proteins were expressed in *E. coli* using an expression system designed by Thony-Meyer *et al*. (1998), and subsequently purified by the use of antibody affinity columns. The electron transfer capabilities of the mutant proteins to metals, including uranium and molybdate, was evaluated by UV spectroscopy and compared to wild-type.

Chapter 2

MATERIALS AND METHODS

I. Bacterial Strains and Plasmids

Desulfovibrio desulfuricans G20 is a strictly anaerobic Gram-negative bacterium, which has a spontaneous mutation that confers nalidixic acid resistance and is cured of the endogenous cryptic plasmid pBG1 (Wall, 1993; Weimer, 1988). Cultures of G20 were grown anaerobically in an undefined medium, designated lactate sulfate (LS) medium. In this medium lactate (60 mM) serves as an electron donor and sodium sulfate (50 mM) serves as the terminal electron acceptor and growth is stimulated by the addition of 1 g Yeast Extract per liter (Rapp, 1987). Manipulations and growth of G20 were carried out in an anaerobic chamber (Coy Laboratory Products, Ann Arbor, MI) with an atmosphere containing nitrogen and a small percentage of hydrogen (<10%).

The *Escherichia coli* strain used as a host for cloning was GC5 Value Efficiency Competent Cells (Gene Choice Inc., Frederick, MD), comparable to DH5α [*end*A1 *rec*A1 *rel*A1 *gyr*A96 *hsd*R17(r_k^-, m_k^+) *pho*A *sup*E44 *thi*-1 Δ(*lac*ZYA-*arg*F)U169 Φ80d*lac*Δ(*lac*Z)M15 F- λ- *ton*A]. The *Escherichia coli* strain used for protein expression was BL21(DE3) (Novagen, San Diego, CA). The BL21(DE3) cells carry a chromosomal copy of the T7 RNA polymerase gene under control of the *lacUV5* promoter [F- *ompT hsdSB* (rb^- mB^-) *gal dcm* (DE3)]. Both *E. coli* strains were grown aerobically at 37°C, with shaking, in LC medium (1% wt/vol tryptone, 0.5% wt/vol yeast extract, 0.5% wt/vol NaCl). Media were solidified by the addition of 1.5% wt/vol agar. Appropriate

antibiotics, added to the media after autoclaving, were ampicillin (100 μg/ml), kanamycin (50 μg/ml), or chloramphenicol (30 μg/ml).

II. Construction of Expression Plasmids

The pET9a vector for protein expression was obtained from Novagen (Figure 2.1). This basic vector contains a T7 promoter for expression of cloned genes and confers kanamycin resistance. Resulting proteins may be unfused or fused with an N-terminal T7 Tag epitope depending on the restriction site utilized for gene insertion. In this work it was decided to isolate unfused proteins by inserting the *cycA* gene at the *NdeI* restriction site.

The wild-type *cycA* gene was amplified by polymerase chain reaction (PCR) from purified G20 genomic DNA,\ utilizing *cycA* PCR primers purchased from Integrated DNA Technologies (Coralville, IA) (Figure 2.2), and the resulting PCR product was cloned into the pGEM-T Easy vector (Promega Corp., Madison, WI). Promega Wizard Genomic DNA Purification Kit (Promega Corp.) was used to isolate G20 genomic DNA. Plasmid DNA preps were performed with the QIAprep Spin Miniprep Kit (Qiagen Inc., Santa Clara, CA). PCR amplification was performed in an Eppendorf thermal cycler (Hamburg, Germany). The 50 μl reaction contained: 1 ng genomic DNA, 20 pmol of each primer, 100 μM dNTP (Invitrogen, Carlsbad, CA), 1 μl pfu polymerase (Stratagene, La Jolla, CA), and 5 μl 10x pfu polymerase buffer. The PCR program was as follows: 1 cycle (95˚C, 1 min.), 30 cycles (95˚C, 30 sec.; 53˚C, 30 sec.; 72˚C, 1 min.), and a final cycle (72˚C, 2 min.). The DNA Core Facility of the University of Missouri provided DNA sequencing services to sequence the cloned fragments and verify that the amplified gene was free of PCR errors. The gene was subcloned into the pET9a vector in the *NdeI*

Figure 2.1. pET9a expression vector (Source: EMD Biosciences Novagen catalog# 69431-3). The gene encoding cytochrome c_3, *cycA*, was cloned into the pET9a expression vector in the *NdeI* site, to create pETc_3. The pETc_3 plasmid was used as a template for site-directed mutagenesis and as the source of wild-type protein for purification.

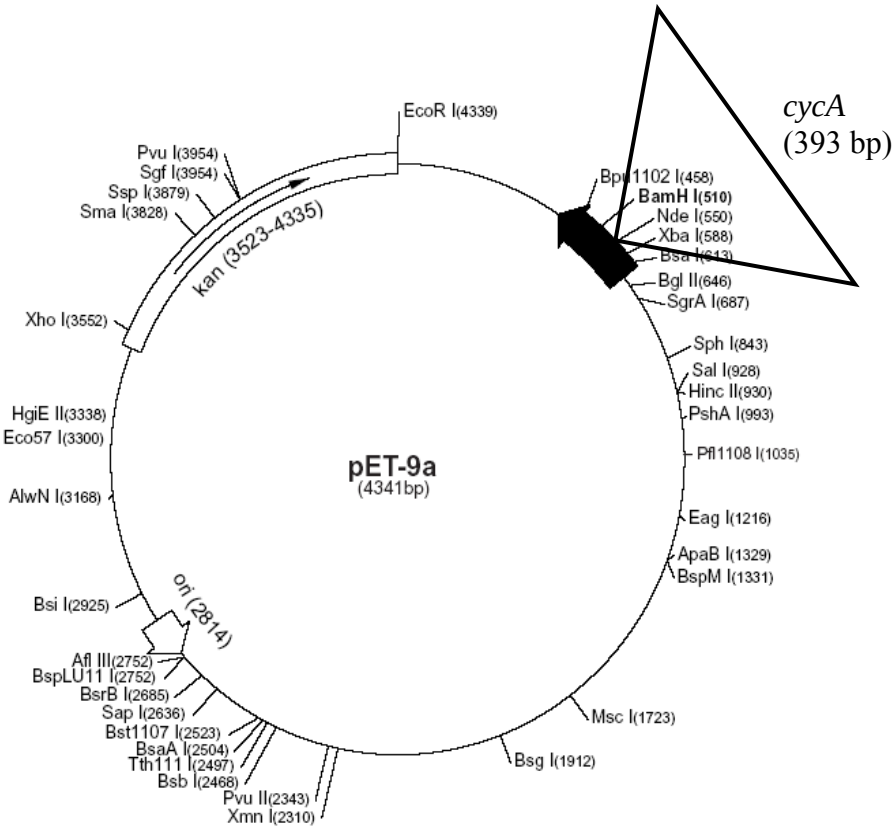

pET-9a sequence landmarks	
T7 promoter	615-631
T7 transcription start	614
T7•Tag coding sequence	519-551
T7 terminator	404-450
pBR322 origin	2814
kan coding sequence	3523-4335

Figure 2.2. DNA sequence of the region of the wild-type *cycA* gene. PCR primers for *cycA* amplification are underlined and shown below.

cycA DNA sequence

gaaaaaatac cgctgagccg gacacggcgc aggcatttgc gctttgcacg ccgcgcaatgcagcctgcgc ggcccgccgc

aggtacgcgc aggctgcccc cccgcgggca cagcgcaggtcatgccccgc aaggtcgctt gcacttttt tcacgcgcag

acccttgct aacctgcgcccctgcttgac agaagtgggg tgtagctcta ggattgccca aattatttaa cataccttgt

signal sequence

gaaggaggta tcacagtt **at gaggaaatcg ctgtttgccg t**aatggtgct ggcactggta gccgcttttg

cycA start

cgctgcccgt gatcgcc gcg gaagcacctg ccgacggtct gaagatggaaaacaccaaaa tgccggtgat cttcaaccac

tccagccact ccagctacca gtgcgccgactgccaccacc ccgttaacgg caaggaaaat cttgccaagt gtgccaccgc

cggctgtcacgatgtttttg acaagaagga caagtctgtc cattcttact acaaaatcat ccacgacagaaaggccacca

ctgttgccac ctgtatgtcc tgccaccttg aagctgcagg cagcgacaag gacctgaaaa aggaactgac cggttgcaaa

cycA end

aagtccaagt gccaccccta g gcactggtccggatttgct tgttcgaggc cgcccgaaag ggcggcctct tgc

Wild-type *cycA* PCR primers

cycA_nde_fwd	CAT ATG AGG AAA TCG CTG TTT GCC GT
cycA_nde_rev	CAT ATG CTA GGG GTG GCA CTT GGA CTT

restriction site using protocols given by restriction enzyme manufacturers (Promega Corp.) (Figure 2.1).

III. Site-Directed Mutagenesis

Site-directed mutations were created according to kit instructions using QuikChange XL Site-Directed Mutagenesis kit (Stratagene). Mutagenic primers were designed to encompass 10-15 base pairs on either side of the amino acid to be mutated (Table 2.1). The pET9a plasmid containing the wild-type *cycA* gene, pETc_3, was used as a template in the mutant strand synthesis reaction. The synthesis was carried out in an Eppendorf thermal cycler as directed in the mutagenesis protocol given by Stratagene. Following mutant strand synthesis and amplification, the reaction was digested with *DpnI* (provided in kit) to eliminate the methylated template plasmid. Plasmids containing desired mutations were transformed, by heat shock, into *E. coli* GC5 Value Efficiency Competent Cells (Gene Choice Inc.) by the procedures provided by the supplier of the competent cells. DNA sequencing performed by the University of Missouri DNA Core Facilities verified incorporation of the specific mutations.

To express the CycA protein in *E. coli*, pET-c_3 or derivative plasmids (conferring kanamycin resistance) containing the wild-type or mutant genes, respectively, were co-transformed with the plasmid pEC86 (Arslan, 1998) (Figure 2.3). The latter encodes cytochrome maturation genes of *E. coli* and confers chloramphenicol resistance. Plasmids were simultaneously electroporated with the Electro Square Porator ECM 830 (BTX, Orlando, FL) set at 330V and 30 ms, into electrocompetent *E. coli* BL21(DE3) cells. After a one hour recovery, the transformants were plated on medium containing kanamycin and chloramphenicol to select for cotransformation.

Table 2.1. Mutagenic PCR primers used for site-directed mutagenesis of *cycA.*

Mutation	Primer	Primer DNA Sequence	Plasmid Name
F19A	F19A forward primer	GCC GGT GAT C**GC C**AA CCA CTC CAG CC	pETc_3-F19A
	F19A reverse primer	GGC TGG AGT GGT T**GG C**GA TCA CCG GC	
Y27A	Y27A forward primer	AGC CAC TCC AGC **GCC** CAG TAC GCC GAC	pETc_3-Y27A
	Y27A reverse primer	GTC GGC GTA CTG **GGC** GCT GGA GTG GCT	
C45A	C45A forward primer	AAT CTT GCC AAG **GCA** GCC ACC GCC GGC	pETc_3-C45A
	C45A reverse primer	GCC GGC GGT GGC **TGC** CTT GGC AAG ATT	
K66A	K66A forward primer	CAA GTC TGT CCA TTC TTA CTA C**GC A**AT CAT CCA CGA CAG AAA GGC CAC C	pETc_3-K66A
	K66A reverse primer	GGT GGC CTT TCT GTC GTG GAT GAT **TGC** GTA GTA AGA ATG GAC AGA CTT G	
K70A	K70A forward primer	CTA CAA AAT CAT CCA CGA CAG A**GC G**GC CAC CAC TGT TGC CAC CTG TAT G	pETc_3-K70A
	K70A reverse primer	CAT ACA GGT GGC AAC AGT GGT GGC **CGC** TCT GTC GTG GAT GAT TTT GTA G	
M80K	M80K forward primer	GGC CAC CAC TGT TGC CAC CTG T**AA A**TC CTG CCA CCT TGA AGC TGC AG	pETc_3-M80K
	M80K reverse primer	CTG CAG CTT CAA GGT GGC AGG A**TT T**AC AGG TGG CAA CAG TGG TGG CC	
K14A	K14A forward primer	GAC GGT CTG AAG ATG GAA AAC ACC **GCA** ATG CCG GTG ATC TTC AAC CAC TCC	pETc_3-K14A
	K14A reverse primer	GGA GTG GTT GAA GAT CAC CGG CAT **TGC** GGT GTT TTC CAT CTT CAG ACC GTC	

*Nucleotides in bold indicate mutations created

Figure 2.3. Plasmid pEC86 containing cytochrome maturation genes and encoding chloramphenicol resistance (Arslan, 1998).

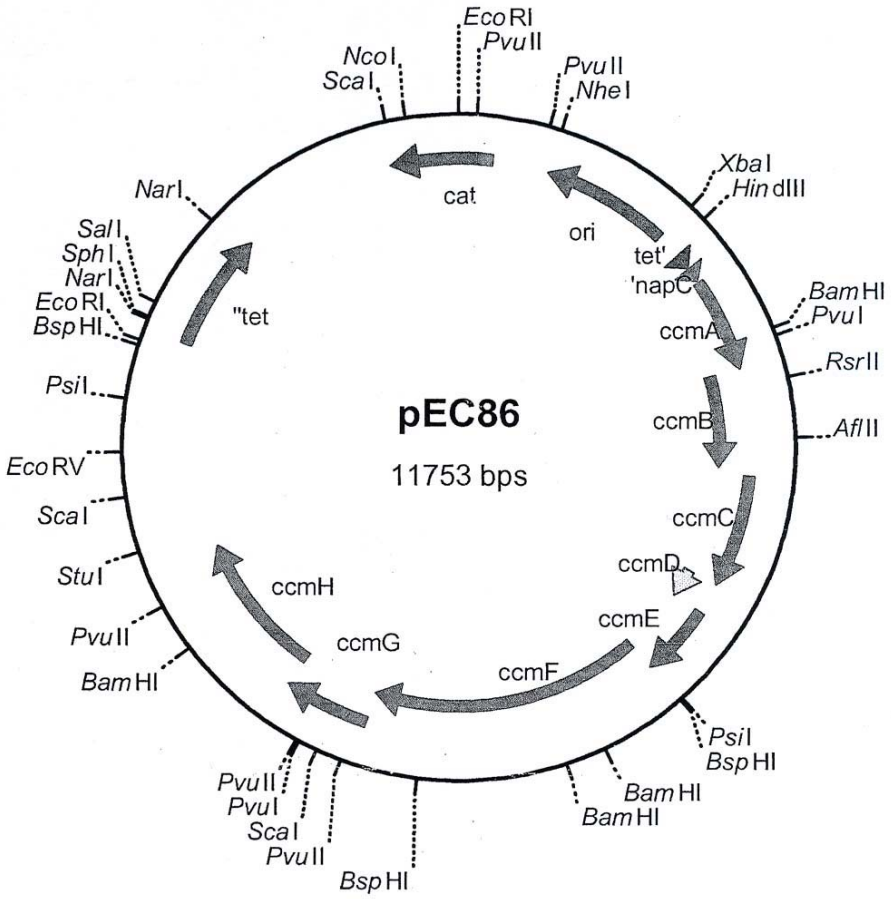
pEC86
11753 bps
cat
ori
tet'
'napC
ccmA
ccmB
ccmC
ccmD
ccmE
ccmF
ccmG
ccmH
"tet
EcoRI
PvuII
NcoI
ScaI
PvuII
NheI
XbaI
HindIII
BamHI
PvuI
RsrII
AflII
PsiI
BspHI
BamHI
BamHI
PsiI
BspHI
PvuII
PvuI
ScaI
PvuII
BspHI
PvuII
BamHI
StuI
ScaI
EcoRV
PsiI
BspHI
EcoRI
NarI
SphI
SalI
NarI

IV. Production and Purification of Proteins

A. Protein Analysis

SDS-PAGE followed by protein staining with Coomassie, heme staining, or Western blot analysis were used routinely to examine purified cytochromes. Protein extracts and purified fractions were mixed with an equal volume of dissociation buffer (8 M Urea, 4% wt/vol SDS, 4% vol/vol β-mercaptoethanol, 2% wt/vol bromophenol blue) and heated in a 65˚C water bath for 30 min. For treatment of pelleted inclusion bodies, pelleted material was mixed with an equal volume of dissociation buffer, heated in a 65˚C water bath for 30 min, centrifuged (13000 x *g* for 2 min.), and the supernatant applied to the gel. Samples were loaded onto a 12.5% wt/vol acrylamide separation gel with 3% wt/vol acrylamide in the stacking gel. Running buffer was Tris (3.3 g/l), glycine (14.4 g/l), and SDS (1 g/l). Typically three identical gels were run simultaneously such that one could be Coomassie stained, one heme stained, and a third transferred to nitrocellulose for subsequent Western blot analysis. Gels to be Coomassie stained were immersed and gently rocked in Coomassie stain solution (0.1% wt/vol Coomassie BB R-250, 7% vol/vol acetic acid, 50% vol/vol methanol) for about one hour and were destained by immersion and gentle rocking in Coomassie destain solution (7% vol/vol acetic acid, 20% vol/vol methanol, 3% glycerol) overnight. Gels to be heme stained were immersed and gently rocked in 50 ml of freshly prepared heme staining solution (20 mg of tetramethyl benzidine, 15 ml methanol, 35 ml 0.25 M sodium acetate pH 5) for 30 min. in the dark. Fresh hydrogen peroxide (5 ml) was added and rocking continued until the desired intensity of bands was attained (Goodhew, 1986; Thomas, 1976). Lastly, Western blot analysis was performed following transfer to 0.45 μm-pore sized

nitrocellulose membrane (Osmonics Inc., Minnetonka, MN). Cytochrome c_3 was detected by the use of cytochrome c_3 specific polyclonal antibody (see below) and anti-rabbit IgG (alkaline phosphatase-conjugated) as a secondary antibody (Sigma-Aldrich Co., St. Louis, MO). Membranes were washed as follows: Phosphate Buffered Saline (PBS) (16% wt/vol NaCl, 0.4% wt/vol KH_2PO_4, 2.3% wt/vol Na_2HPO_4, 0.4% wt/vol NaN_3, 0.4% wt/vol KCl, pH 7.2), 0.3% wt/vol tween (PBS-tween), 2 times 5 min. each; PBS-tween + NaCl (1 M), 2 times 5 min. each; PBS-tween, 3 times 5 min. each; PBS, 5 min.; Buffer pH 9.5 (100 mM Tris, 100 mM NaCl, 5 mM $MgCl_2$, pH 9.5), 2 times 5 min. each. Membranes were developed with BCIP (5-Bromo-4-Chloro-3'-Indolyphosphate p-Toluidine Salt) and NBT (Nitro-Blue Tetrazolium Chloride) (Sigma Aldrich) according to manufacturers instructions. Bradford assays, using purified bovine serum albumin as a standard, were used routinely to quantitate purified proteins (Bradford, 1976). In all protein gels, standards were either MultiMark Multi-Colored Standard (Invitrogen, Carlsbad, CA) or ProSieve Color Protein Markers (Cambrex, East Rutherford, NJ) and a volume of 10 μl was applied.

B. Antibody Production

The immunology services of Covance Research Products (Denver, PA) were employed to generate polyclonal antibody specific to purified CycA. Protein was purified from G20 as previously described (Van Der Westen, 1978). Approximately 2 mg of protein was required to complete antibody production. Purified protein, followed by several boosts, was inoculated into rabbits and serum was collected. IgG was purified from serum by Covance Research Products. Covance also tested the anti-CycA IgG for specificity by ELISA assay.

C. Antibody Affinity Column Assembly

To purify wild-type and mutant cytochromes c_3 by affinity chromatography, CycA-specific antibodies were cross-linked to CNBr-activated sepharose 4B (Fischer Scientific, Hampton, NH) in glass columns (27 ml volume, 15 cm length) (BioRad Laboratories, Hercules, CA). Immunopure Binding Buffer and Immunopure Elution Buffer, proprietary reagents were used for protein purification (Pierce Biotechnology Inc., Rockford, IL). Briefly, the CNBr resin was activated by an acid rinse with 200 ml 1mM HCl per gram of resin. The activated resin was collected by vacuum on a sintered glass filter and thoroughly rinsed with cold (about 4˚C) water. In this study 9 mg of IgG was used per ml of resin, slightly below maximum binding capacity of 10 mg per ml of resin. Antibody was immobilized to the resin overnight at 4°C. Resin (4 ml) with immobilized antibody was loaded into a column and the void volume was collected for SDS-PAGE analysis to verify that the antibody had crosslinked to the resin. Any remaining unbound active sites in the resin were blocked by passing an excess of 0.75 M glycine/1.5 M NaCl buffer through the column. Subsequently, the column was washed with Immunopure Elution Buffer followed by Immunopure Binding Buffer. Anti-CycA sepharose columns were stored at 4˚C in Immunopure Binding Buffer containing 0.2% wt/vol sodium azide to prevent bacterial growth. Separate columns were prepared for the purification of the wild-type and each of the mutant CycA proteins.

D. Protein Expression

E. coli BL21(DE3) cells co-transformed with plasmids pEC86 and pET9a vector containing the wild-type or mutant genes were grown overnight in LC medium with appropriate antibiotics, kanamycin (50 μg/ml) and chloramphenicol (30 μg/ml) (Arslan,

1998). Overnight cultures (50 ml) were subcultured into fresh LC medium (1 liter) containing antibiotics. Cultures were grown to an $OD_{600\ nm}$ of 0.5, generally requiring 2-3 hours, IPTG was added to a final concentration of 1 mM, and cells were incubated for a further 4 hours. Following this induction, *E. coli* was harvested by centrifugation (4000 x *g* for 20 minutes at 4˚C) and the pellet was resuspended in 10 ml buffer (100 mM TrisHCl, 150 mM NaCl, 1 mM EDTA pH 8.0). Resuspended cells were sonicated with a Branson Digital Sonifier (VWR Scientific, West Chester, PA), 10 sec. on/20 sec. off (chilled on ice), for a total of 2 min. then centrifuged (13000 x *g* for 1 h at 4˚C) and the supernatant collected in a clean test tube. This *E. coli* lysate was analyzed by SDS-PAGE followed by Coomassie staining, heme staining, and Western blot analysis to check for the presence of CycA proteins.

E. Antibody Affinity Protein Purification

The *E. coli* cell lysate prepared as described above (generally about 10-15 ml per liter of culture) was placed on an anti-CycA sepharose column. Void volume was retained to verify by protein analysis that protein was captured on the column. Columns were then washed with 30 column volumes of Immunopure Binding Buffer and the protein was eluted from the column with 20 ml of Immunopure Elution Buffer. Eluted fractions were pooled and dialyzed overnight against 4 liters Phosphate Buffered Saline (16% wt/vol NaCl, 0.4% wt/vol KH_2PO_4, 2.3% wt/vol Na_2HPO_4, 0.4% wt/vol NaN_3, 0.4% wt/vol KCl, pH 7.2). All steps of protein purification and dialysis were performed at 4˚C and all reagents were previously chilled. Eluted proteins were concentrated using Centriplus YM-10 centrifugal devices (Millipore Corp., Billerica, MA) and were

analyzed by SDS-PAGE followed by protein staining, heme staining, and Western blotting to verify purity and identity.

Several high molecular weight contaminants were found to be present following antibody affinity column purification. These were removed by a subsequent purification step that utilized Centriplus YM-50 centrifugal filtration devices obtained from Millipore Corp. This filtration device allows passage of low molecular weight proteins into the lower reservoir, while retaining higher molecular weight proteins in the upper reservoir. Centrifugal filtration was carried out as indicated in the instructions provided. Following filtration, purity was again assessed by protein analysis as described above. It was observed that the CycA protein passed through the YM-50 filter while the higher molecular weight contaminants were successfully retained by this separation step.

V. Spectrophotometric Analysis

Spectrophotometric analysis was performed on a Cary 1 Bio UV-visible spectrophotometer (Varian Inc., Palo Alto, CA). Prior to analysis, Tris buffer (10 mM, pH 7.6) was prepared, aliquoted (about 10 ml aliquots), sealed in Hungate tubes (Bellco, Vineland, NJ), and deoxygenated by bubbling with nitrogen gas for approximately two hours. A solution of sodium dithionite (100 mM) was prepared the day of use in deoxygenated Tris buffer. Uranyl acetate (10 mM) and sodium molybdate (20 mM) solutions were also prepared in deoxygenated Tris buffer. Uranyl bicarbonate (10 mM) was prepared by adding uranyl acetate to freshly prepared deoxygenated bicarbonate buffer (30 mM). Purified proteins, generally 0.5-1.0 μM concentration, were placed into screw-capped sealable quartz cuvettes (Starna Cells Inc., Atascadero, CA) containing 1 ml of deoxygenated Tris buffer. Characteristic absorption spectra were recorded for the

oxidized proteins from 350 to 600 nm. Sodium dithionite in 60 molar excess of the protein concentration was added to reduce the proteins. The absorption spectra for the reduced proteins were recorded. Excess dithionite was titrated by further additions of purified protein, typically about 0.25-1.0 μM of purified protein. The progress of the titration was followed with additional spectra readings and was continued until there was no further detectable increase in the absorbance at $A_{418\ nm}$, the maximum absorbance for the reduced cytochrome. Uranium and molybdate in 2-3 molar excess of the protein concentration were added to the reduced protein. The absorption spectra for the reduced proteins with metals were similarly recorded from 350 to 600 nm.

Chapter 3

RESULTS

I. Cytochrome c_3 Protein Expression

In order to express and purify wild-type and mutant CycA proteins, a suitable protein expression system was required. Overproduction of *c*-type cytochromes has previously been limited due to the inability to mature the apoprotein and provide sufficient hemes in *E. coli* (Voordouw, 1990). Production of mature cytochrome proteins requires the presence of specific chaperones and transporters necessary for translocation of the precursor protein and heme into the periplasm, and for the incorporation of heme into the apoprotein. This obstacle has been overcome by co-transforming the plasmid pEC86, containing cytochrome maturation genes, and the expression vector containing the cytochrome genes (Arslan, 1998).

Protein expression was induced and cells were harvested and sonicated. Following centrifugation of lysed cells, a distinct color difference in the cell lysate supernatant of the cultures cotransformed with plasmid pEC86 and the pETc_3 expression vector was observed when compared to a lysate obtained from control cultures lacking both plasmids (Figure 3.1). Pink color, a consequence of cytochrome expression, was present in both the induced and uninduced cell cultures cotransformed with both plasmids. Both the supernatant and pellet preparations were collected and analyzed by SDS-PAGE followed by Coomassie staining, heme staining, and Western blot analysis (Figure 3.2). The tetraheme cytochrome c_3 protein was present in the soluble fraction of the cell preparation at the predicted molecular weight of 13 kDa in the case of wild-type

Figure 3.1. *E. coli* BL21(DE3) lysates collected from cultures IPTG induced and uninduced to express recombinant *D. desulfuricans* G20 tetraheme cytochrome c_3 showing the visible color change accompanying the production of mature, heme containing cytochrome c_3.

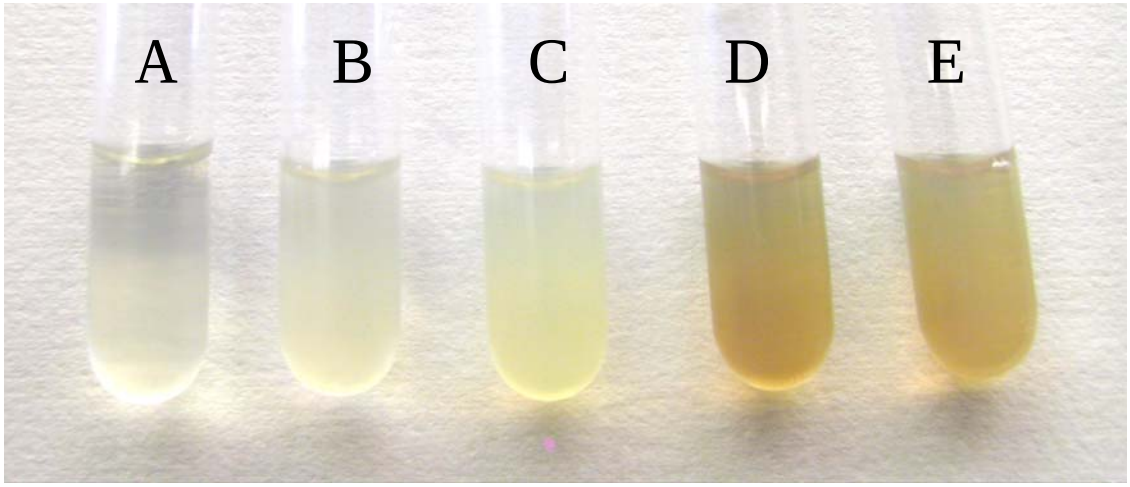

Sample Key

A no plasmid +IPTG

B pET9a vector positive induction control + 1 mM IPTG

C pETc_3 plasmid alone + 1 mM IPTG

D cotransformant pETc_3/pEC86 –IPTG

E cotransformant pETc_3/pEC86 + 1 mM IPTG

Figure 3.2. Protein analysis of *E. coli* BL21(DE3) (pETc_3/pEC86) lysates. A) Coomassie stain, B) heme stain, and C) Western blot analysis is shown for the supernatant and pellet prepared from *E. coli* cells induced or uninduced to express recombinant *D. desulfuricans* G20 cytochrome c_3 protein. Lane 1, MultiMark molecular weight standards; lane 2, purified cytochrome c_3 from *D. desulfuricans* G20; lane 3, *E. coli* BL21(DE3) (pET9a) empty vector control + 1 mM IPTG; lane 4, *E. coli* BL21(DE3) (pETc_3) without pEC86 + 1 mM IPTG; lane 5, *E. coli* BL21(DE3) (pET-28b) + 1 mM IPTG, induction control producing β-galactosidase (119 kDa); lane 6, soluble extract from uninduced (1 mM IPTG) *E. coli* BL21(DE3) (pETc_3/pEC86); lane 7, soluble extract from induced (1mM IPTG) *E. coli* BL21(DE3) (pETc_3/pEC86); lane 8, solubilized pellet from uninduced *E. coli* BL21(DE3) (pETc_3/pEC86); lane 9, solubilized pellet from induced *E. coli* BL21(DE3) (pETc_3/pEC86). Approximately 40 μg of protein was loaded into each lane.

A.

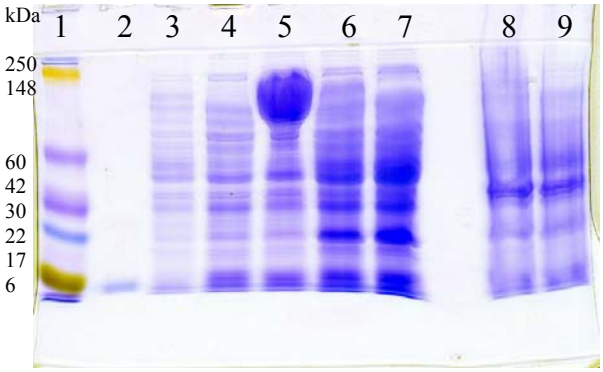
kDa
1 2 3 4 5 6 7 8 9
250
148
60
42
30
22
17
6

B.

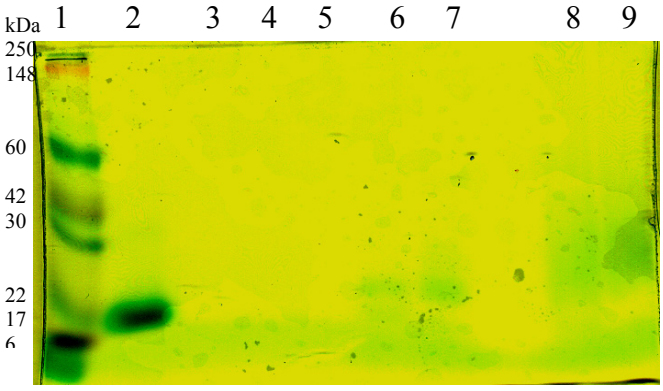
kDa
1 2 3 4 5 6 7 8 9
250
148
60
42
30
22
17
6

C.

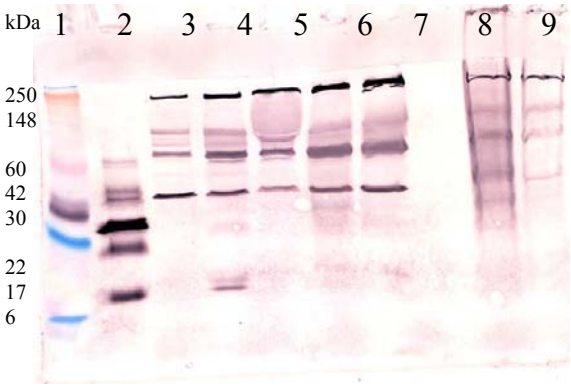
kDa
1 2 3 4 5 6 7 8 9
250
148
60
42
30
22
17
6

and all mutants with the exception of Y27A. The production of the Y27A mutant protein was never detected.

II. Cytochrome c_3 Protein Purification

Wild-type *Desulfovibrio desulfuricans* strain G20 cytochrome c_3 protein was purified from *E. coli* lysate by the use of an anti-CycA sepharose column. Following this initial purification step, the eluted proteins were concentrated and separated by SDS-PAGE followed by Coomassie staining. Several contaminants, of a higher molecular weight than the cytochrome c_3 protein, were present following antibody affinity purification. Therefore, a centrifugal filtration device with a molecular weight cutoff of 50 kDa was employed to separate the cytochrome from the higher molecular weight contaminants (Figure 3.3). Following this secondary purification step, proteins were analyzed by SDS-PAGE followed by Coomassie staining, heme staining, and Western blotting to verify identity and purity. It appeared that the high molecular weight contaminants were retained in the upper reservoir of the Centriplus column, while the CycA protein was able to pass into the lower reservoir. Subsequently, purification of mutant proteins was performed in the same manner (Figures 3.4-3.6).

Figure 3.3. SDS-PAGE separation of proteins stained with Coomassie of immunoaffinity purified recombinant *D. desulfuricans* G20 cytochrome c_3 before and after centrifugation filter treatment. Lane 1, recombinant wild-type cytochrome c_3 eluted from the immunoaffinity column; lane 2, recombinant cytochrome after removal of high molecular weight proteins by filtration; lane 3, purified native *D. desulfuricans* G20 cytochrome c_3; lane 4, MultiMark protein standard. Protein quantity in each lane was roughly 1-2 μg.

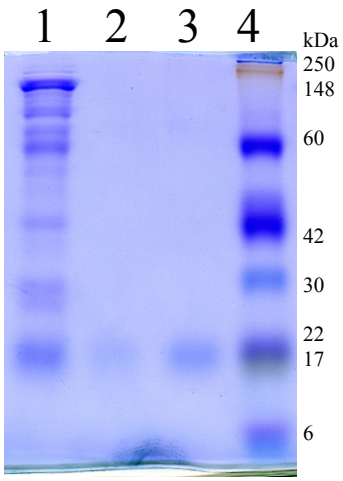
1
2
3
4
kDa
250
148
60
42
30
22
17
6

Figure 3.4. Protein analysis of immunoaffinity purified recombinant *D. desulfuricans* G20 cytochrome c_3 F19A mutant and C45A mutant. A) Western blot analysis, B) Coomassie stain, and C) heme stain is shown. Lane 1, MultiMark protein molecular weight standards; lane 2, purified cytochrome c_3 F19A mutant (3.3 μg); lane 3, purified cytochrome c_3 C45A mutant (1.5 μg); lane 4, purified cytochrome c_3 from *D. desulfuricans* G20 (2 μg).

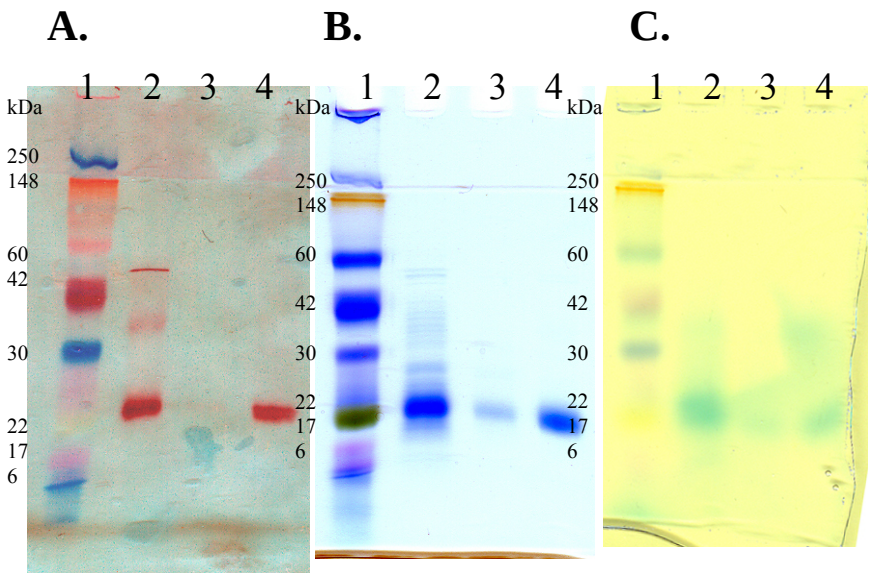
A.
B.
C.
1 2 3 4
kDa
250
148
60
42
30
22
17
6

Figure 3.5. Protein analysis of immunoaffinity purified recombinant *D. desulfuricans* G20 cytochrome c_3 K66A mutant and K72A mutant. A) Western blot analysis, B) Coomassie stain, and C) heme stain is shown. Lane 1, MultiMark protein molecular weight standards; lane 2, purified cytochrome c_3 from *D. desulfuricans* G20 (4 μg); lane 3, purified bovine serum albumin (BSA) (2 μg); lane 4, purified cytochrome c_3 K66A mutant (1 μg); lane 5, purified cytochrome c_3 K72A mutant (0.5 μg).

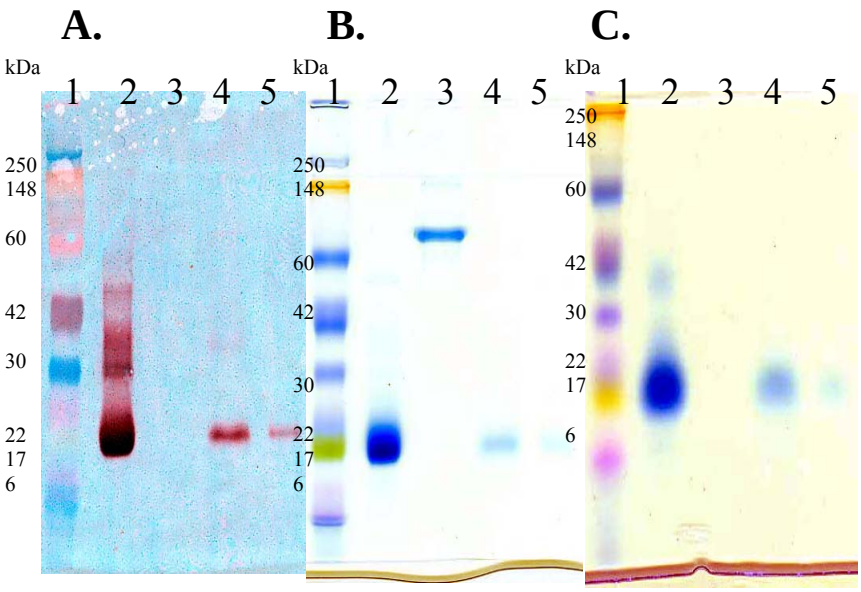
A.
B.
C.
kDa
1 2 3 4 5
250
148
60
42
30
22
17
6

Figure 3.6. Protein analysis of immunoaffinity purified recombinant *D. desulfuricans* G20 cytochrome c_3 M80K mutant and K14A mutant. A) Western blot analysis, B) Coomassie stain, and C) heme stain is shown. Lane 1, ProSieve protein molecular weight standards; lane 2, purified cytochrome c_3 M80K mutant (3 μg); lane 3, purified cytochrome c_3 K14A mutant (3 μg); lane 4, purified cytochrome c_3 from *D. desulfuricans* G20 (2 μg).

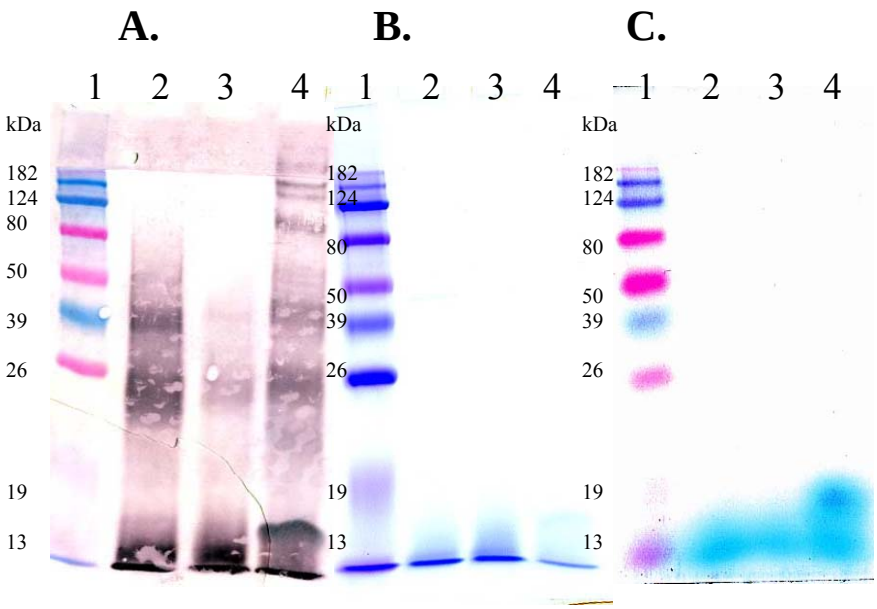
A.
B.
C.
1 2 3 4
1 2 3 4
1 2 3 4
kDa
182
124
80
50
39
26
19
13
kDa
182
124
80
50
39
26
19
13
kDa
182
124
80
50
39
26
19
13

III. Oxidation of Reduced Cytochrome c_3 with U(VI)

To determine whether the mutant versions of CycA were impaired in their ability to reduce U(VI) to U(IV), functional assays of the cytochromes were carried out. The absorption spectra (350-600 nm) for the wild-type oxidized cytochrome c_3 protein were recorded. Sodium dithionite in 60 molar excess of the protein concentration was added to reduce the protein and the absorption spectra was again recorded. In order to titrate away excess dithionite incremental additions of purified protein were added (about 1 μM), followed by additional spectra readings, until there was no increase detected in the absorbance of the reduced peak. Uranyl acetate, in 2-3 molar excess of the protein concentration, was added to the reduced protein and the absorption spectrum for the reduced protein with uranium was recorded. It was observed that the wild-type reduced cytochrome c_3 protein was oxidized by the addition of uranium (Figure 3.7). The absorption spectra for the mutant proteins oxidized, reduced, and following the addition of uranyl acetate were recorded in a similar manner (Figure 3.8-3.13). All mutants were reoxidized upon addition of uranyl acetate to the reduced proteins. Results are summarized in Table 3.1.

Figure 3.7. Oxidation of reduced recombinant *D. desulfuricans* cytochrome c_3 by the addition of uranyl acetate. Green spectrum, oxidized unmutated cytochrome c_3 protein (1.5 μM); blue spectrum, cytochrome reduced by the addition of sodium dithionite (75 μM); red spectrum, cytochrome oxidized by the addition of uranyl acetate to the reduced cytochrome (4 μM).

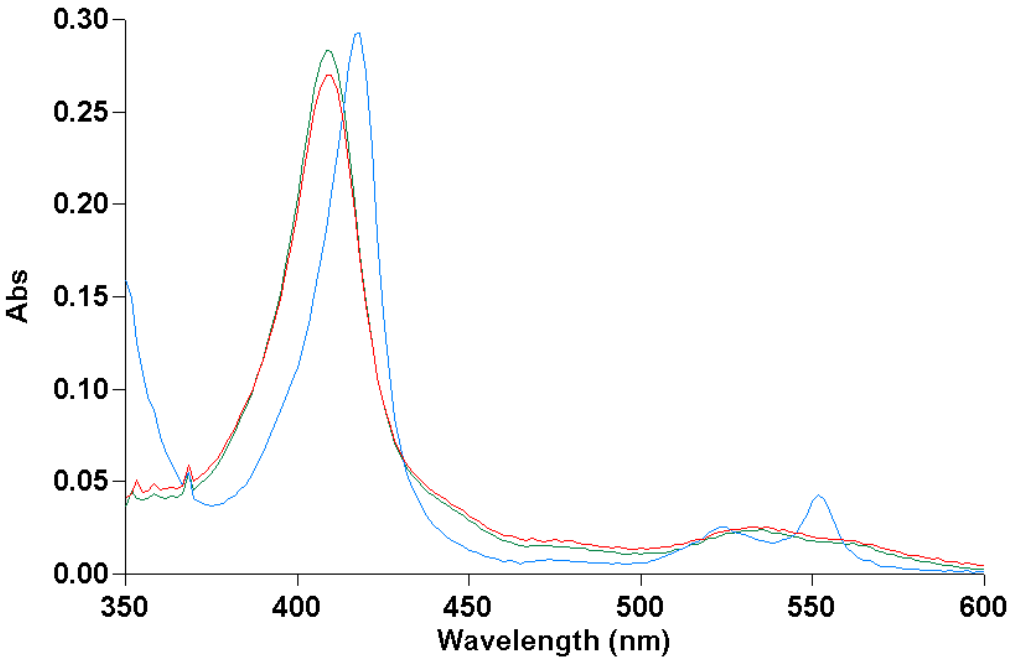
0.30
0.25
0.20
0.15
0.10
0.05
0.00
Abs
350
400
450
500
550
600
Wavelength (nm)

Figure 3.8. Oxidation of reduced recombinant *D. desulfuricans* cytochrome c_3 F19A mutant by the addition of uranyl acetate. Green spectrum, oxidized F19A mutant cytochrome c_3 protein (1.5 μM); blue spectrum, cytochrome reduced by the addition of sodium dithionite (75 μM); red spectrum, cytochrome oxidized by the addition of uranyl acetate to the reduced cytochrome (4 μM).

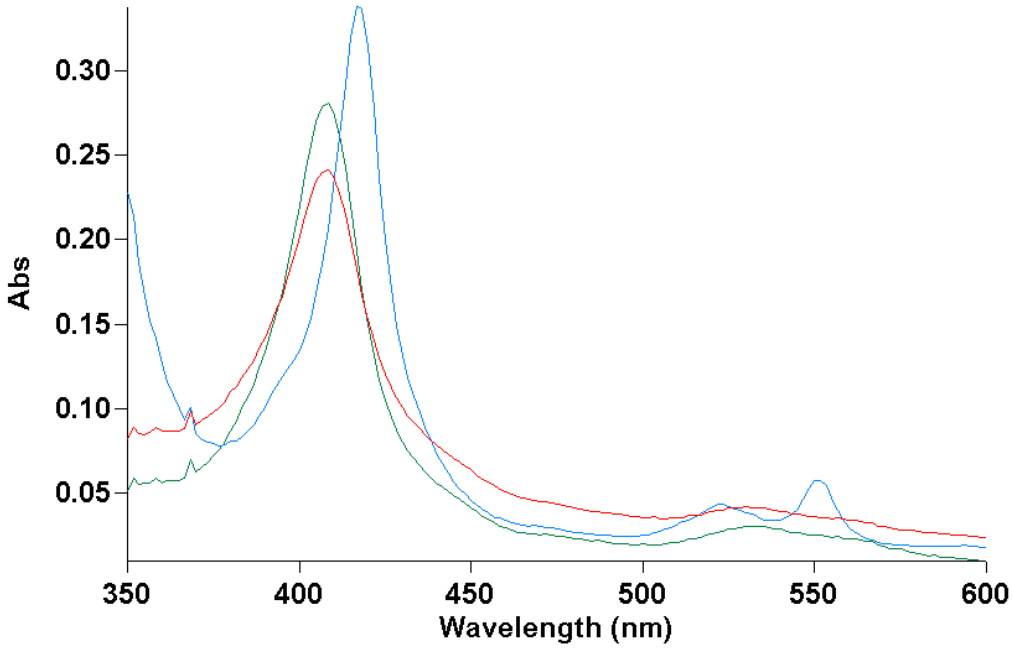
0.30
0.25
0.20
0.15
0.10
0.05
Abs
350
400
450
500
550
600
Wavelength (nm)

Figure 3.9. Oxidation of reduced recombinant *D. desulfuricans* cytochrome c_3 C45A mutant by the addition of uranyl acetate. Green spectrum, oxidized C45A mutant cytochrome c_3 protein (1.2 μM); blue spectrum, cytochrome reduced by the addition of sodium dithionite (75 μM); red spectrum, cytochrome oxidized by the addition of uranyl acetate to the reduced cytochrome (4 μM).

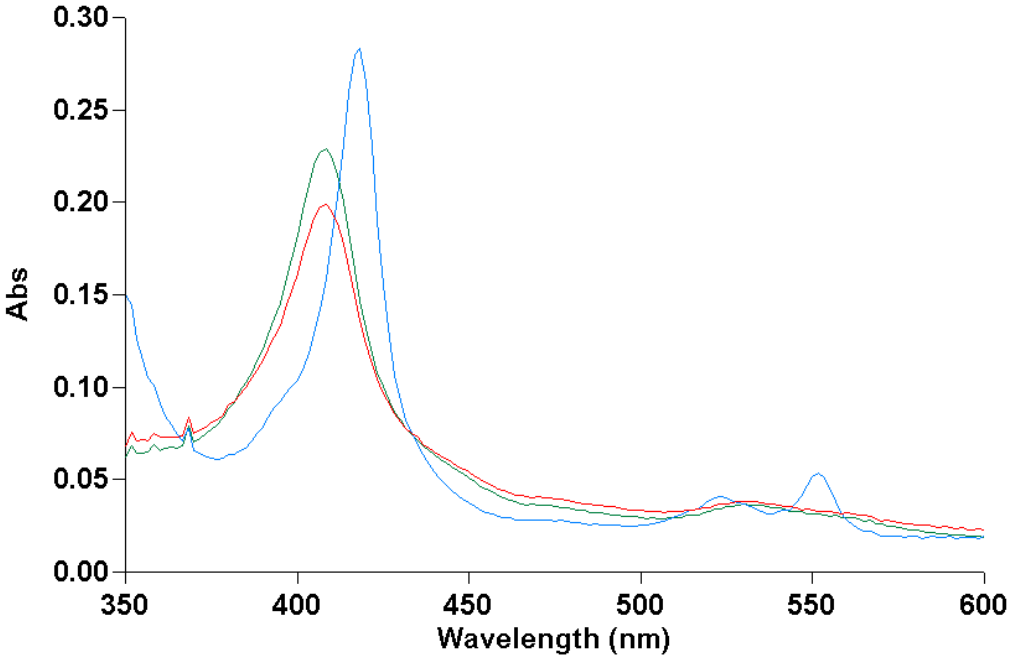
0.30
0.25
0.20
0.15
0.10
0.05
0.00
Abs
350
400
450
500
550
600
Wavelength (nm)

Figure 3.10. Oxidation of reduced recombinant *D. desulfuricans* cytochrome c_3 K66A mutant by the addition of uranyl acetate. Green spectrum, oxidized K66A mutant cytochrome c_3 protein (2.6 μM); blue spectrum, cytochrome reduced by the addition of sodium dithionite (75 μM); red spectrum, cytochrome oxidized by the addition of uranyl acetate to the reduced cytochrome (6 μM).

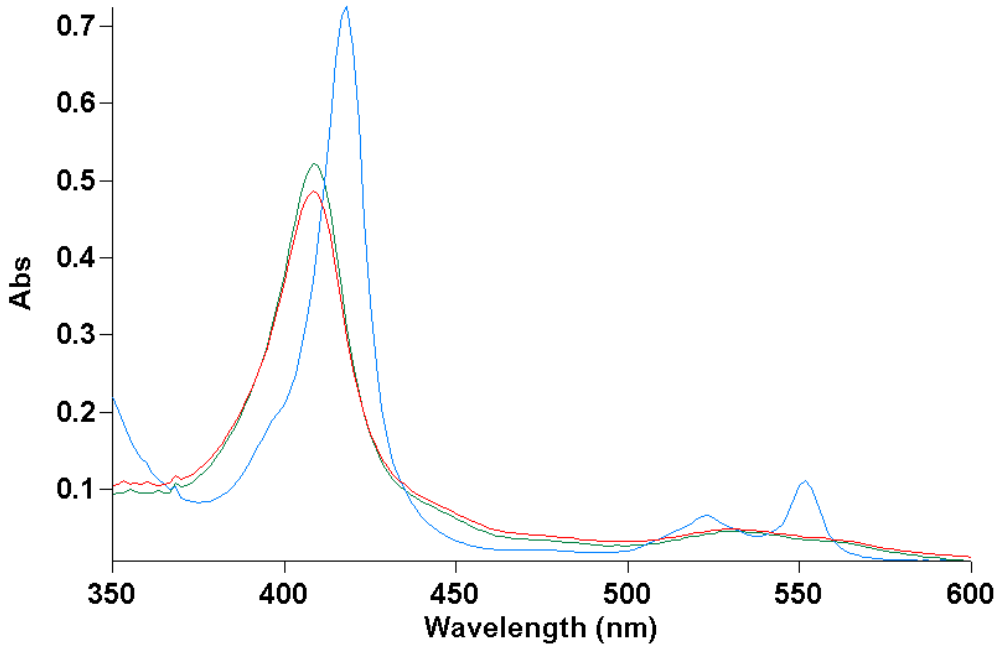
0.7
0.6
0.5
0.4
0.3
0.2
0.1
Abs
350
400
450
500
550
600
Wavelength (nm)

Figure 3.11. Oxidation of reduced recombinant *D. desulfuricans* cytochrome c_3 K72A mutant by the addition of uranyl acetate. Green spectrum, oxidized K72A mutant cytochrome c_3 protein (1.9 μM); blue spectrum, cytochrome reduced by the addition of sodium dithionite (75 μM); red spectrum, cytochrome oxidized by the addition of uranyl acetate to the reduced cytochrome (6 μM).

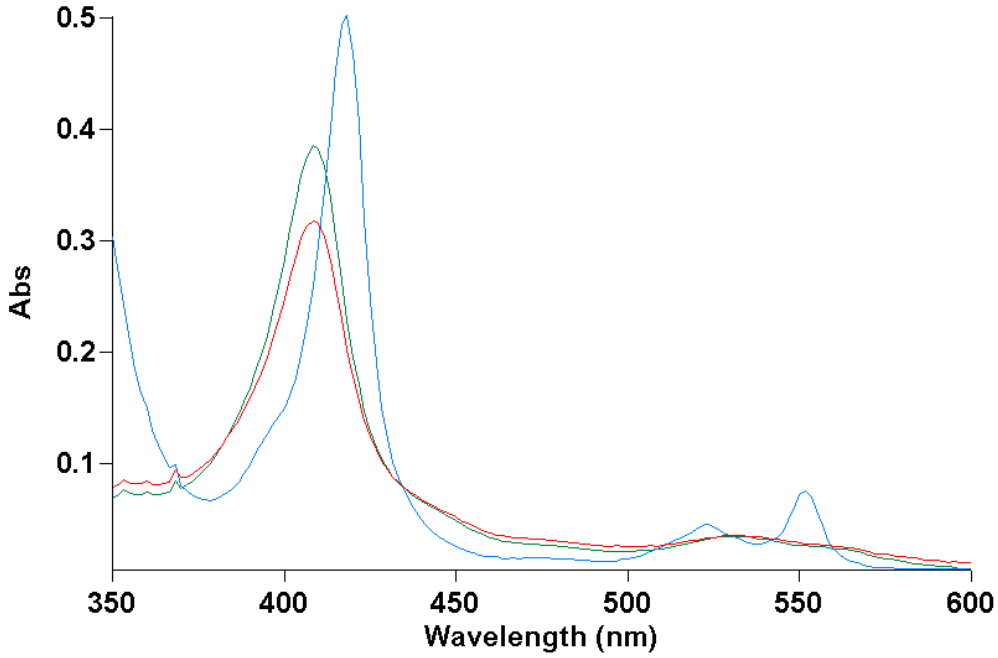
0.5
0.4
0.3
0.2
0.1
Abs
350
400
450
500
550
600
Wavelength (nm)

Figure 3.12. Oxidation of reduced recombinant *D. desulfuricans* cytochrome c_3 M80K mutant by the addition of uranyl acetate. Green spectrum, oxidized M80K mutant cytochrome c_3 protein (1.6 μM); blue spectrum, cytochrome reduced by the addition of sodium dithionite (75 μM); red spectrum, cytochrome oxidized by the addition of uranyl acetate to the reduced cytochrome (4 μM).

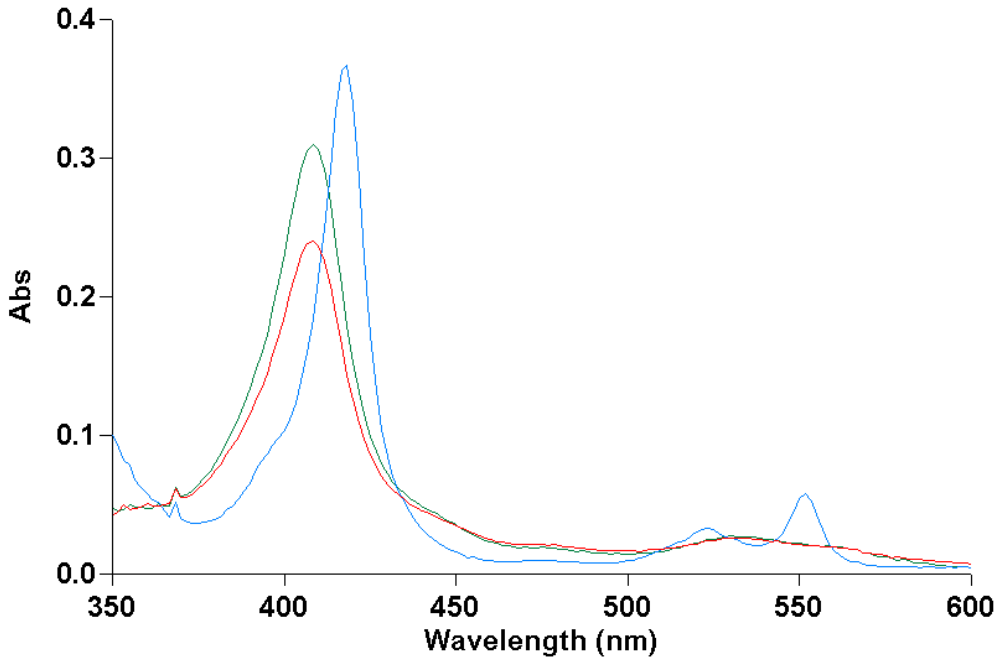
0.4
0.3
0.2
0.1
0.0
Abs
350
400
450
500
550
600
Wavelength (nm)

Figure 3.13. Oxidation of reduced recombinant *D. desulfuricans* cytochrome c_3 K14A mutant by the addition of uranyl acetate. Green spectrum, oxidized K14A mutant cytochrome c_3 protein (1.2 μM); blue spectrum, cytochrome reduced by the addition of sodium dithionite (75 μM); red spectrum, cytochrome oxidized by the addition of uranyl acetate to the reduced cytochrome (4 μM).

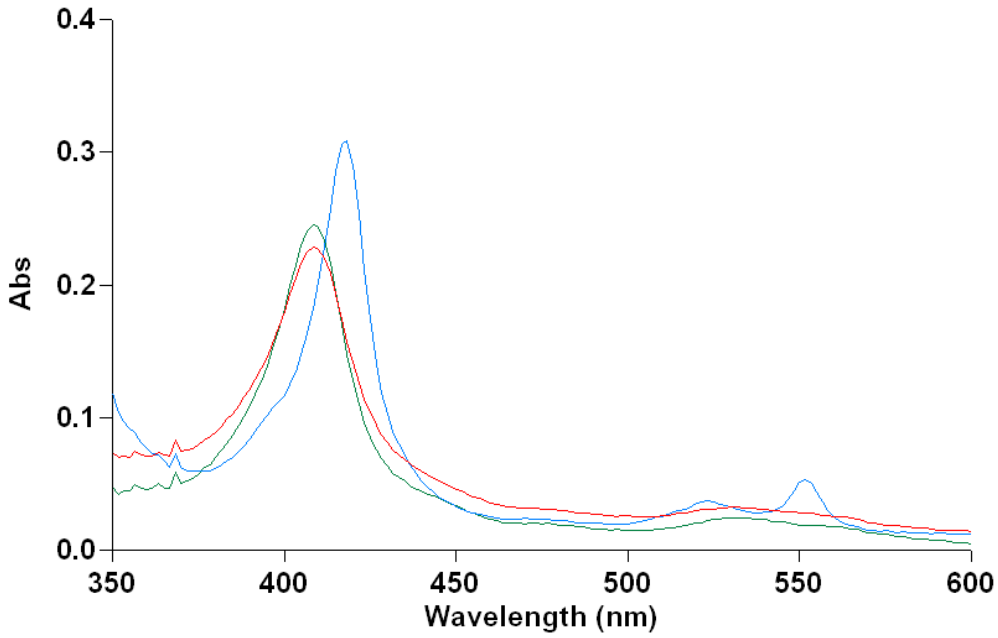
0.4
0.3
0.2
0.1
0.0
Abs
350
400
450
500
550
600
Wavelength (nm)

Table 3.1. Summary of UV spectroscopic analyses of non-mutant and mutant tetraheme cytochrome c_3 from *D. desulfuricans* oxidized by uranyl acetate.

Sample	Total Protein Concentration (μM)	Uranyl Acetate Concentration (μM)	Protein Re-oxidized
wild-type	1.5	4	yes
F19A	1.5	4	yes
C45A	1.2	4	yes
K66A	2.6	6	yes
K72A	1.9	6	yes
M80K	1.6	4	yes
K14A	1.2	4	yes

IV. Oxidation of Reduced Cytochrome c_3 with Mo(VI)

The ability of molybdate to oxidize the reduced tetraheme cytochrome c_3 mutants was tested in a similar fashion to U(VI). The absorption spectrum (350-600 nm) for the wild-type oxidized cytochrome c_3 protein was recorded. Sodium dithionite in 60 molar excess of the protein concentration was added to reduce the protein and the absorption spectra was again recorded. Excess dithionite was titrated using further additions of purified protein until there was no significant increase in the absorbance of the reduced peak. This was followed by the addition of sodium molybdate in 2-3 molar excess of protein concentration. The absorption spectrum for the protein following molybdate addition was recorded. It was observed that the reduced wild-type cytochrome c_3 protein was oxidized by the addition of molybdate (Figure 3.14). The absorption spectra for the mutant proteins were recorded in a similar manner (Figures 3.15-3.20). All mutants, with the exception of K14A, were reoxidized similarly to wild-type upon the addition of molybdate. The K14A mutant was unable to be reoxidized, even when 100 μM of molybdate was added (Figure 3.20). This result implies that this residue may represent a critical point for interaction and electron transfer between the cytochrome c_3 protein and molybdate. Results from studies with molybdate are summarized in Table 3.2.

Figure 3.14. Oxidation of reduced recombinant *D. desulfuricans* cytochrome c_3 by the addition of sodium molybdate. Green spectrum, oxidized unmutated cytochrome c_3 protein (1.5 μM); blue spectrum, cytochrome reduced by the addition of sodium dithionite (75 μM); red spectrum, cytochrome oxidized by the addition of sodium molybdate to the reduced cytochrome (3 μM).

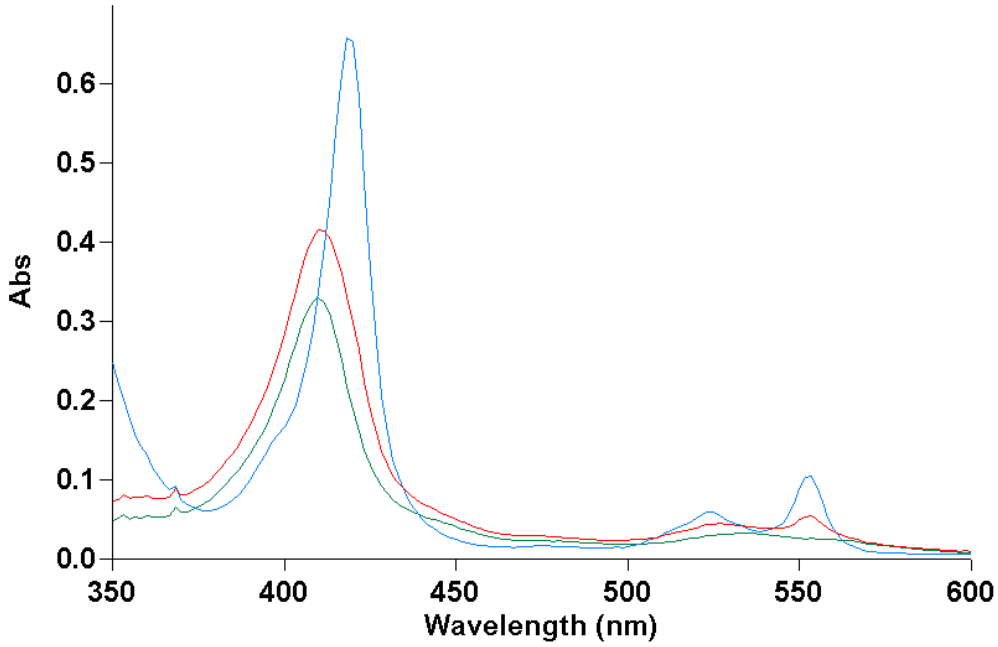
Abs
0.0
0.1
0.2
0.3
0.4
0.5
0.6
350
400
450
500
550
600
Wavelength (nm)

Figure 3.15. Oxidation of reduced recombinant *D. desulfuricans* cytochrome c_3 F19A mutant by the addition of sodium molybdate. Green spectrum, oxidized F19A mutant cytochrome c_3 protein (1.2 μM); blue spectrum, cytochrome reduced by the addition of sodium dithionite (75 μM); red spectrum, cytochrome oxidized by the addition of sodium molybdate to the reduced cytochrome (4 μM).

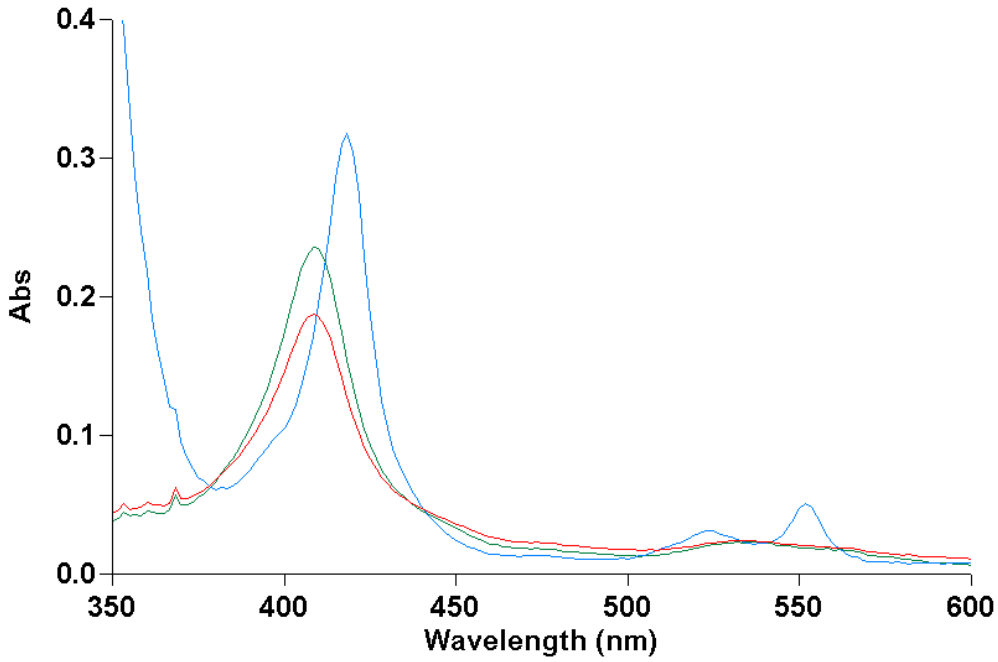
0.4
0.3
0.2
0.1
0.0
Abs
350
400
450
500
550
600
Wavelength (nm)

Figure 3.16. Oxidation of reduced recombinant *D. desulfuricans* cytochrome c_3 C45A mutant by the addition of sodium molybdate. Green spectrum, oxidized C45A mutant cytochrome c_3 protein (1.5 μM); blue spectrum, cytochrome reduced by the addition of sodium dithionite (75 μM); red spectrum, cytochrome oxidized by the addition of sodium molybdate to the reduced cytochrome (4 μM).

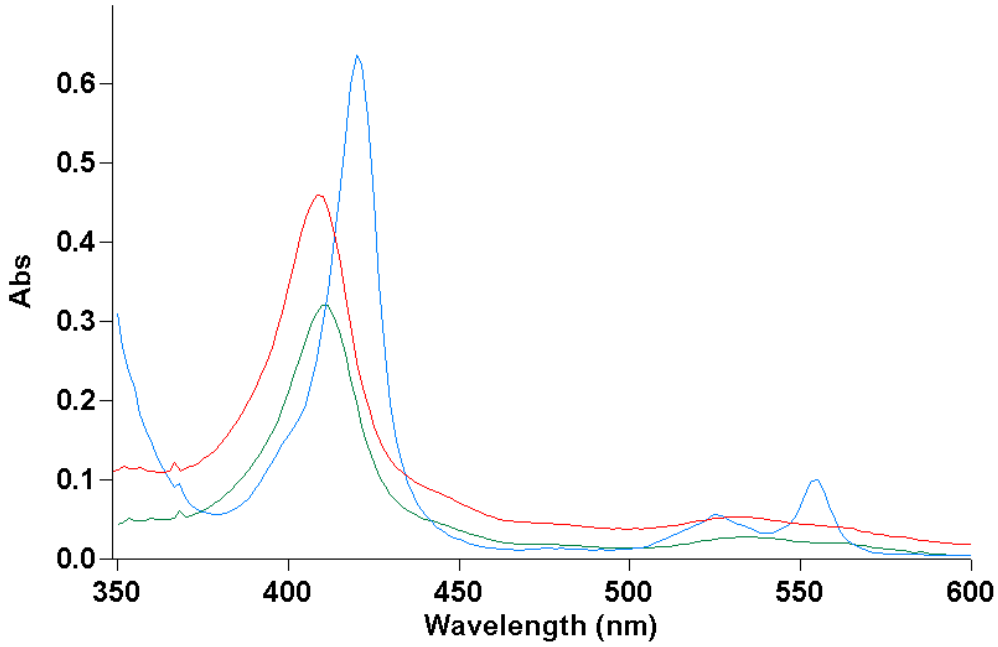
Abs
0.0
0.1
0.2
0.3
0.4
0.5
0.6
350
400
450
500
550
600
Wavelength (nm)

Figure 3.17. Oxidation of reduced recombinant *D. desulfuricans* cytochrome c_3 K66A mutant by the addition of sodium molybdate. Green spectrum, oxidized K66A mutant cytochrome c_3 protein (.75 μM); blue spectrum, cytochrome reduced by the addition of sodium dithionite (75 μM); red spectrum, cytochrome oxidized by the addition of sodium molybdate to the reduced cytochrome (3 μM).

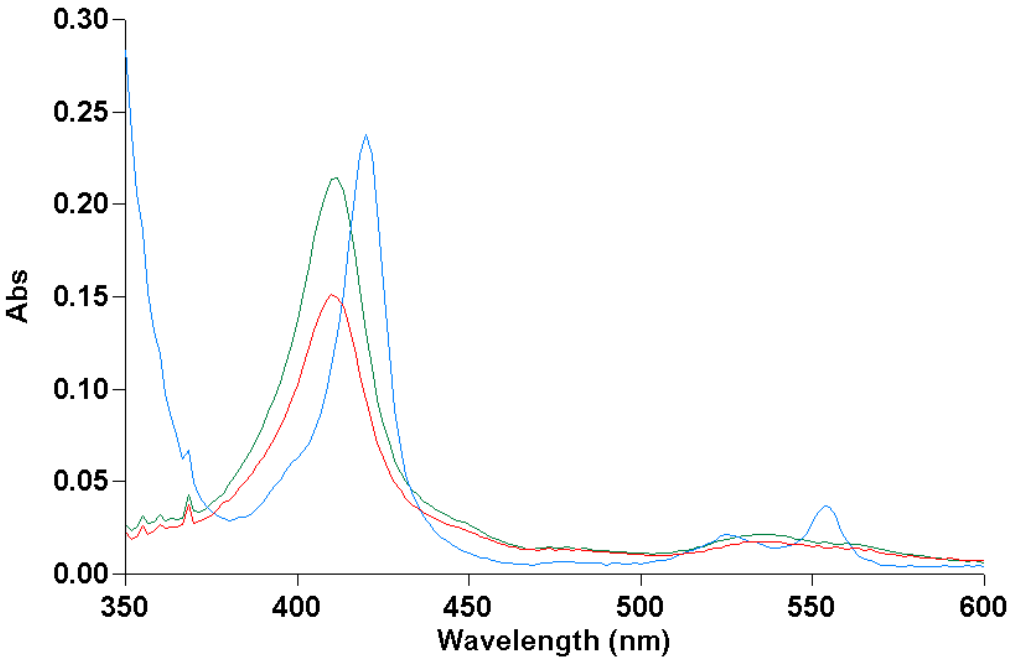
0.30
0.25
0.20
0.15
0.10
0.05
0.00
Abs
350
400
450
500
550
600
Wavelength (nm)

Figure 3.18. Oxidation of reduced recombinant *D. desulfuricans* cytochrome c_3 K72A mutant by the addition of sodium molybdate. Green spectrum, oxidized K72A mutant cytochrome c_3 protein (1.5 μM); blue spectrum, cytochrome reduced by the addition of sodium dithionite (75 μM); red spectrum, cytochrome oxidized by the addition of sodium molybdate to the reduced cytochrome (3 μM).

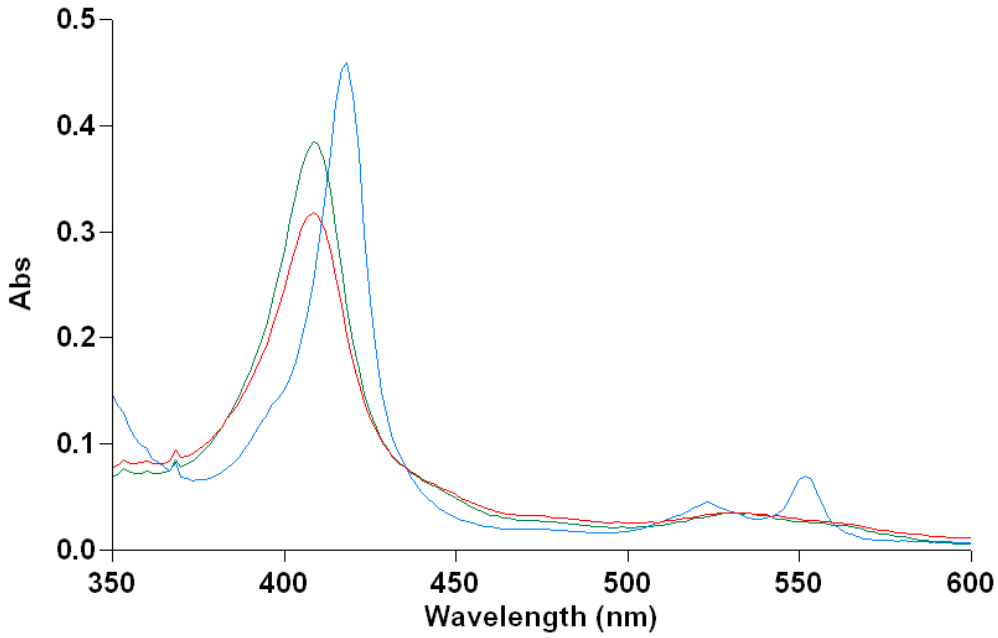
0.5
0.4
0.3
0.2
0.1
0.0
Abs
350
400
450
500
550
600
Wavelength (nm)

Figure 3.19. Oxidation of reduced recombinant *D. desulfuricans* cytochrome c_3 M80K mutant by the addition of sodium molybdate. Green spectrum, oxidized M80K mutant cytochrome c_3 protein (1.7 μM); blue spectrum, cytochrome reduced by the addition of sodium dithionite (75 μM); red spectrum, cytochrome oxidized by the addition of sodium molybdate to the reduced cytochrome (4 μM).

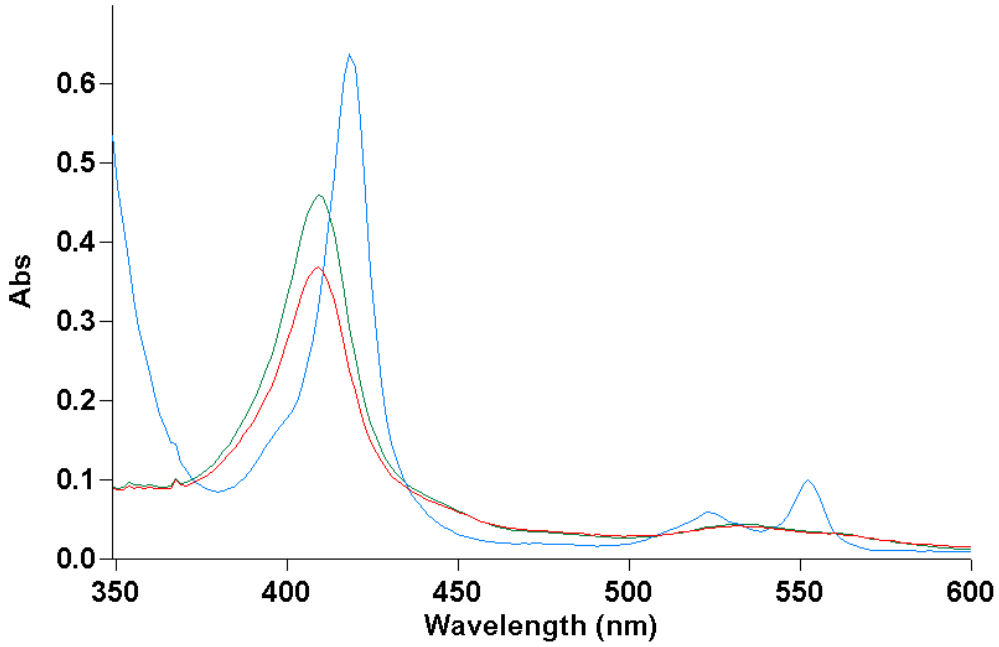
Abs
0.0
0.1
0.2
0.3
0.4
0.5
0.6
350
400
450
500
550
600
Wavelength (nm)

Figure 3.20. Spectra of reduced recombinant *D. desulfuricans* cytochrome c_3 K14A mutant following the addition of sodium molybdate. Green spectrum, oxidized K14A mutant cytochrome c_3 protein (2 μM); black spectrum, cytochrome reduced by the addition of sodium dithionite (75 μM); purple spectrum, addition of sodium molybdate to the reduced cytochrome (5 μM); pink spectrum, addition of sodium molybdate to the reduced cytochrome (10 μM); blue spectrum, addition of sodium molybdate to the reduced cytochrome (25 μM); red spectrum, addition of sodium molybdate to the reduced cytochrome (100 μM).

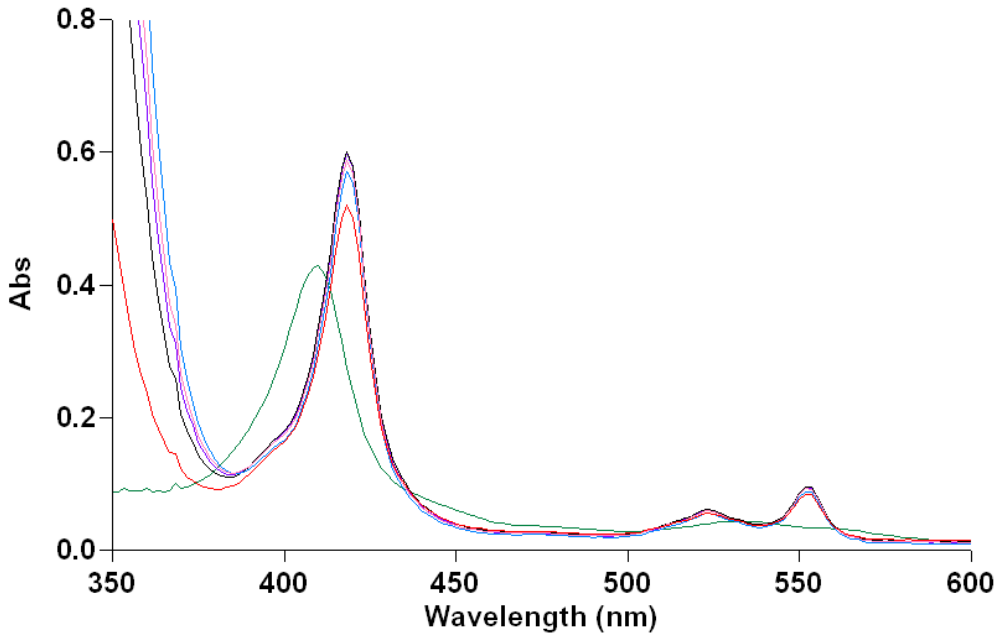
0.8
0.6
0.4
0.2
0.0
Abs
350
400
450
500
550
600
Wavelength (nm)

Table 3.2. Summary of UV spectroscopic analyses of non-mutant and mutant cytochrome c_3 from *D. desulfuricans* oxidized by sodium molybdate.

Sample	Total Protein Concentration (μM)	Molybdate Concentration (μM)	Protein Re-oxidized
wild-type	1.5	3	yes
F19A	1.2	4	yes
C45A	1.5	4	yes
K66A	0.75	3	yes
K72A	1.5	3	yes
M80K	1.7	4	yes
K14A	2	up to 100	no

V. Cytochrome c_3 Interaction with Uranyl Carbonate

The cytochrome c_3 K14A reduced protein was unable to be oxidized by the addition of Mo(VI) as the negatively charged molybdate ion, although it was oxidized by the addition of U(VI) as uranyl acetate. Experiments were conducted to determine whether this mutant protein could transfer electrons to U(VI) if the uranyl ion were complexed with carbonate forming a negatively charged species (Ganesh, 1997). Similarly to uranyl acetate, uranyl carbonate was added to the reduced protein and absorption spectra recorded to determine if uranium in this form were able to oxidize the reduced wild-type and K14A mutant protein. It was found that both the non-mutant and K14A mutant reduced proteins were reoxidized by the addition of uranyl carbonate (Figure 3.21-3.22).

Figure 3.21. Oxidation of reduced recombinant *D. desulfuricans* cytochrome c_3 by the addition of uranyl carbonate. Green spectrum, oxidized unmutated cytochrome c_3 protein (1.1 μM); blue spectrum, cytochrome reduced by the addition of sodium dithionite (75 μM); red spectrum, cytochrome oxidized by the addition of uranyl carbonate to the reduced cytochrome (4 μM).

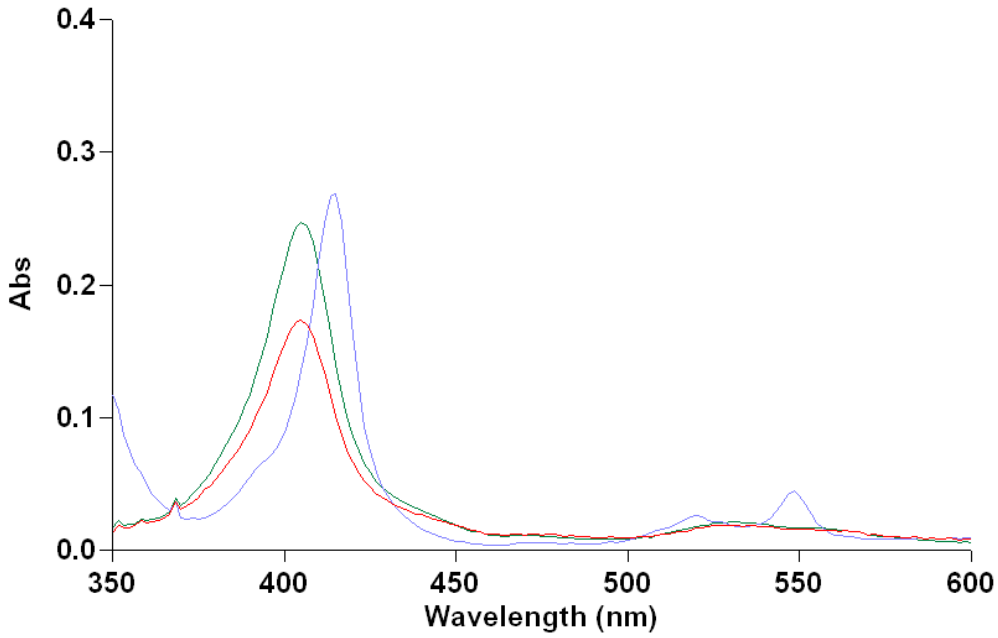
0.4
0.3
0.2
0.1
0.0
Abs
350
400
450
500
550
600
Wavelength (nm)

Figure 3.22. Oxidation of reduced recombinant *D. desulfuricans* cytochrome c_3 K14A mutant by the addition of uranyl carbonate. Green spectrum, oxidized K14A mutant cytochrome c_3 protein (1.0 μM); blue spectrum, cytochrome reduced by the addition of sodium dithionite (75 μM); red spectrum, cytochrome oxidized by the addition of uranyl acetate to the reduced cytochrome (4 μM).

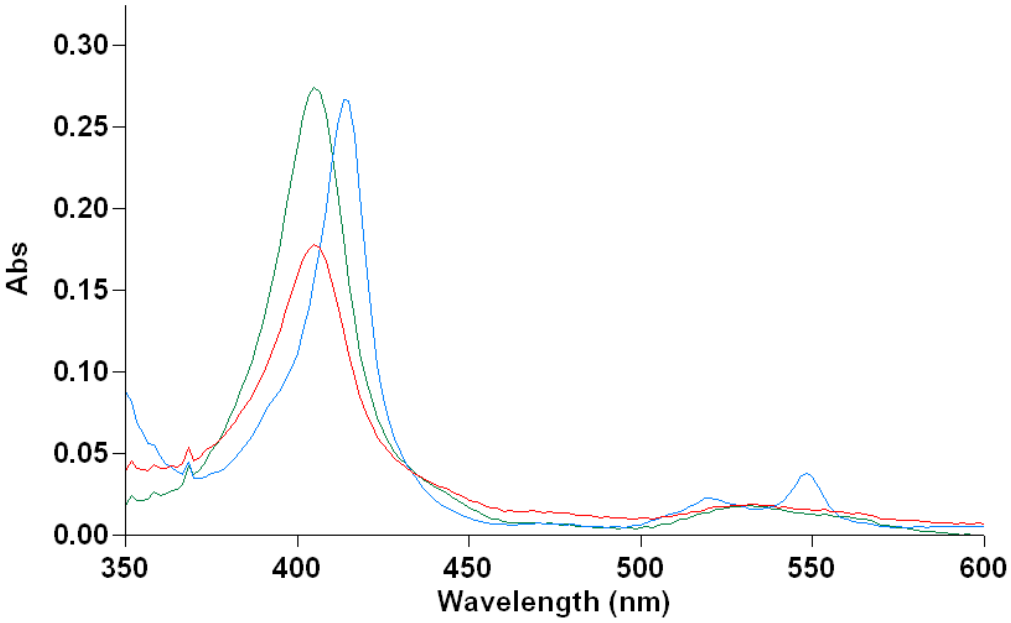
0.30
0.25
0.20
0.15
0.10
0.05
0.00
Abs
350
400
450
500
550
600
Wavelength (nm)

Chapter 4

DISCUSSION

Cytochrome c_3 of the SRB *Desulfovibrio desulfuricans* has been the subject of recent investigations due to its apparent role as a U(VI) reductase and the confirmation of the involvement of this protein in U(VI) reduction by an analysis of a mutant lacking the cytochrome, $CycA^-$ (Aubert, 1998; Payne, 2002). In this study specific amino acid residues of the cytochrome were chosen for mutation. The resulting proteins were purified and compared to the non-mutant cytochrome c_3 to determine how the protein interacts with redox active metals.

In order to purify cytochrome c_3 an efficient and reliable method of protein expression was needed. Cytochrome c_3 is a *c*-type tetraheme cytochrome requiring covalent attachment of each of its four hemes through two thioester bonds to cysteines. Previous attempts to overexpress these proteins in *E. coli* had not been successful. The post-translational maturation is a complex process shown to require increased expression of the *ccm* gene cluster in *E. coli* (Thony-Meyer, 2002). This gene cluster, which encodes functions for transport of hemes to the periplasm and functions for covalent attachment to the apoprotein, has been cloned onto a plasmid, pEC86. When this plasmid was co-transformed with an expression vector containing a *c*-type cytochrome gene in *E.coli*, efficient expression of mature cytochrome protein was achieved (Arslan, 1998). This expression system was successfully utilized in this investigation. It was observed that when the tetraheme cytochrome c_3 was expressed the *E. coli* pellet was distinctively pink compared to uninduced cultures. The expression technique was reproducible and enabled expression in easily cultivatable *E. coli*.

Crystallization studies of the cytochrome c_3 with molybdate have enabled prediction of several amino acid residues that may be important for interaction and electron transfer to metals (Pattarkine *et al.*, manuscript in preparation). The molybdate ion co-crystallized with cytochrome c_3 in the vicinity of heme 4 (Pattarkine *et al.*, manuscript in preparation), and in this study charged residues near the surface proximal edge of heme 4 were chosen for mutagenesis. Other studies have explored the importance of various amino acids in the intraprotein electron transfer as well as in interprotein reductions. Evidence was obtained for a critical role for other conserved residues in electron transfer but it was not always clear whether these residues were important for structure or function. Phenylalanine 20 has been identified as a critical residue for electron flow between hemes within the type 1 cytochrome c_3 in *D. vulgaris* strain Hildenborough (Dolla, 1999; Takayama, 2004). Ozawa *et al.* (2003) observed differences in the rate of reduction of the cytochrome as a result of replacing the aromatic residue tyrosine 43 with a neutral non-aromatic residue. In this study tyrosine 27 was replaced with alanine. Lastly, cysteine 45 was chosen for mutation in order to eliminate the function of heme 2. The tri-heme cytochrome c_7 of *Desulfuromonas acetoxidans* naturally lacks heme 2 and functions as an electron-transfer protein in sulfate reduction (Pereira, 1997).

The ability to observe the oxidation and reduction of cytochromes by UV spectroscopy provides a preliminary mechanism to characterize the electron transfer capabilities of cytochrome mutants. Cytochromes typically have three absorption peaks the α (550 nm), β (521 nm), and the Soret (415 nm) and are often named for the characteristic α absorption wavelength. The Soret peak of oxidized cytochromes has a

typical red shift observed when the cytochrome is reduced by the addition of sodium dithionite. Wild-type cytochrome c_3 has been shown to be reoxidized by the addition of metals, such as uranyl acetate and, remarkably, molybdate. When molybdate was used as a substrate for oxidation of cytochrome c_7 from *Desulfuromonas acetoxidans*, no oxidation of the cytochrome was observed (Assfalg et al. 2002). Thus this ion appeared to bind to the protein and was used as a proxy for chromate interaction with that cytochrome.

In this investigation, recombinant *D. desulfuricans* cytochrome c_3 proteins purified from *E. coli* were found to exhibit the expected absorption spectra for oxidized and reduced proteins. The non-mutant protein was also reoxidized by the addition of uranyl acetate and molybdate. Several mutant tetraheme cytochromes, F19A, C45A, K66A, K72A, and M80K, exhibited no differences from the non-mutant recombinant protein in the absorption spectra of oxidized and reduced proteins with uranyl acetate or molybdate. In contrast, the K14A mutant was not reoxidized when molybdate was added to the reduced protein even when this ion was added in great excess (100 μM). Interestingly the K14A mutant reduced protein was oxidized by the addition of uranyl acetate and uranyl carbonate.

Although differences were not observed in the absorption spectra of several of the cytochrome c_3 mutants, further experiments may reveal important differences in the mutant proteins. Dolla *et al.* (1999) performed UV spectroscopic analysis and kinetic experiments on the F20L mutant of cytochrome c_3 of *D. vulgaris* Hildenborough and found no difference from wild-type, suggesting that the mutation did not effect the interaction and ability to transfer electrons to the cytochrome from the hydrogenase.

However, differences were noted in the process of reduction in the mutant cytochrome compared to wild-type. The mutation appeared to affect the intermolecular cooperativity between cytochromes as deduced by measuring the kinetics of reduction and crystal structure of the mutant. Similarly, it is likely that differences in the F19A mutant of cytochrome c_3 compared to wild-type could be elucidated with such techniques.

The UV spectroscopic analysis of the reduction and oxidation of the cytochrome c_3 K14A mutant has identified lysine 14 as an amino acid critical for electron transfer to molybdate. This positively charged residue, and possibly several other charged residues in close proximity, likely form a binding site for the negatively charged molybdate (Figure 4.1). It is envisioned that electrons are transferred from heme 4 to the metal. These residues form a cleft configuration that may represent the point of interaction with the metal. In order to verify this hypothesis, mutations of lysine residues 56 and 57 would be necessary. Especially interesting was the continued ability of U(VI) to oxidize the K14A mutant cytochrome. Since the uranyl ion (UO_4^{2+}) is positively charged, one might predict an alternate site of interaction of this ion with the reduced cytochrome c_3. The results of differential K14A cytochrome oxidation confirmed this prediction.

Figure 4.1. *D. desulfuricans* type 1 tetraheme cytochrome c_3 structure (Pattarkine et al., in preparation) with heme positions indicated and with residues potentially interacting with metal highlighted. Three charged residues, lysine 14, lysine 56, and lysine 57, were predicted to interact with metals, such as molybdate, and to transfer electrons to heme 4.

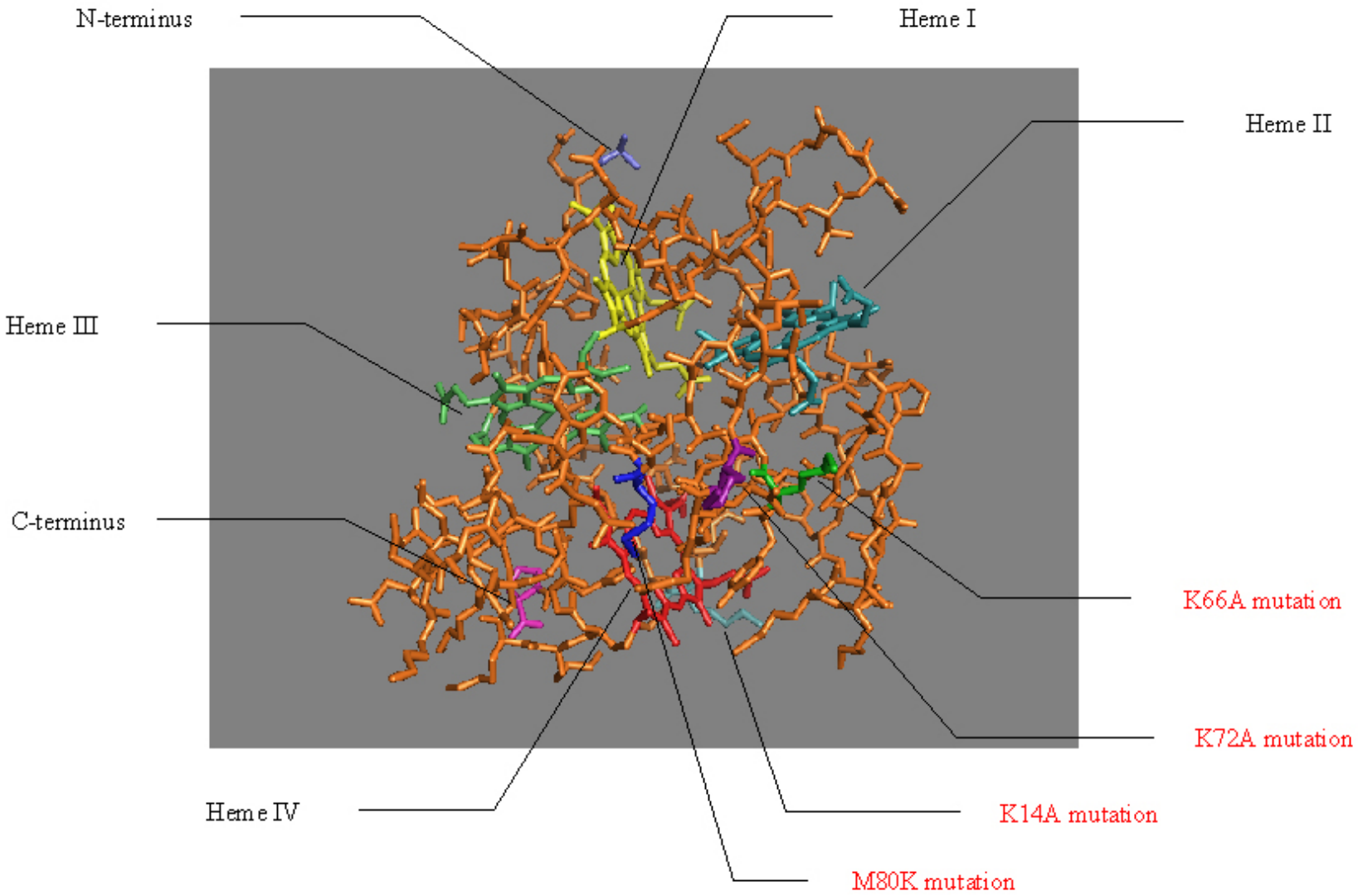
N-terminus
Heme I
Heme II
Heme III
C-terminus
K66A mutation
K72A mutation
Heme IV
K14A mutation
M80K mutation

Interestingly it was found that Y27A cytochrome c_3 production could not be detected in the *E. coli* BL21(DE3) cells nor could the mutant protein be recovered by immunoaffinity chromatography. It is unclear why this expression was not possible. This amino acid could be critical for the structural integrity of the cytochrome or may have a role in the folding of the molecule.

It was also predicted that the C45A mutation might prevent proper attachment of heme groups to the protein. Although no changes in the size of the protein were observed, there were differences in the expression and purification of this mutant. The distinctive pink color was not present in the C45A mutant *E. coli* pellet or lysate. However, despite the possible loss of one or more hemes in this mutant, electron transfer to uranyl acetate and molybdate was evident by UV spectroscopy. It is also possible that the C45A mutation has not eliminated heme 2 from the molecule but rather it remains tethered. In this case it might be expected that the heme would be less tightly bound generating a broader peak in the heme absorption spectra. To test this, the height of the non-mutant and mutant oxidized peaks were measured and the width of the peak was measured at the point of half of the height, deriving a half-peak width measurement (Table 4.1). It was observed that the C45A mutant had a greater half-peak width than the non-mutant. More precise measurements of the redox activity attained through kinetic studies and also completion of the crystal structure of the C45A mutant would be necessary to better characterize the effect of an apparent loss of the cysteine ligand for heme 2 on the cytochrome function.

Table 4.1. Half peak width measurements of non-mutant and mutant oxidized cytochrome c_3 absorption spectra. Half peak width measurement was calculated by measuring the height of the peak and measuring the width of the peak at the half point.

Sample	Half-peak width 1 (cm)	Half-peak width 2 (cm)	Half-peak width 3 (cm)
non-mutant	1.2	1.35	1.3
F19A	1.5	1.5	
C45A	1.7	1.45	
K66A	1.3	1.3	
K72A	1.35	1.4	
M80K	1.4	1.4	
K14A	1.4	1.4	1.35

This study has identified at least one critical amino acid residue for electron transfer to molybdate and therefore provides the basis for further research. The precise mechanisms of interaction with metals and electron flow require more detailed analysis. For example kinetic studies of the K14A mutant would provide information about the rate of reduction and oxidation by U(VI). Crystallization studies would give detailed information about the structure of the mutant protein. Lastly, the creation and analysis of other amino acid mutations such as lysine 56 and 57, in the vicinity of heme 4, would more clearly define the point of interaction between cytochrome c_3 and metals.

LITERATURE CITED

Abdelouas, A., M. Fattahi, B. Grambow, L. Vichot, and E. Gautier. 2002. Precipitation of technetium by subsurface sulfate-reducing bacteria. *Radiochimica Acta*: 773-777.

Abdelouas, A., W. Lutze, G. Weiliang, E. H. Nuttall, B. A. Strietelmeier, and B. J. Travis. 2000. Biological reduction of uranium in groundwater and subsurface soil. *The Science of The Total Environment*: 21-35.

Argyle, J. L., B. J. Rapp-Giles, and J. D. Wall. 1992. Plasmid transfer by conjugation in *Desulfovibrio desulfuricans*. *FEMS Microbiol Letters* 73: 255-62.

Arslan, E., H. Schulz, R. Zufferey, P. Kuenzler, and L. Thoney-Meyer. 1998. Overproduction of the *Bradyrhizobium japonicum c*-type cytochrome subunits of the cbb3 oxidase in *Escherichia coli*. *Biochemical & Biophysical Research Communications* 25: 744-747.

Assfalg, M., I. Bertini, P. Turano, M. Bruschi, M. C. Durand, and A. Dolla. 2002. A quick solution structure determination of the fully oxidized double mutant K9-10A cytochrome c_7 from *Desulfuromonas acetoxidans* and mechanistic implications. *Journal of Biomolecular NMR* 22: 107-122.

Aubert, C., G. Leroy, P. Bianco, E. Forest, M. Bruschi, and A. Dolla. 1998. Characterization of the cytochromes *c* from *Desulfovibrio desulfuricans* G201. *Biochemical & Biophysical Research Communications* 242: 213-218.

Aubert, C., G. Leroy, M. Bruschi, J. D. Wall, and A. Dolla. 1997. A single mutation in the heme 4 environment of *Desulfovibrio desulfuricans* Norway cytochrome c_3 (m-r 26,000) greatly affects the molecule reactivity. *Journal of Biological Chemistry* 272: 15128-15134.

Bradford, M. M. 1976. A rapid and sensitive method for the quantitation of microgram quantities of protein utilizing the principle of protein-dye binding. *Analytical Biochemistry*: 248-254.

Da Costa, P. N., C. Conte, and L. M. Saraiva. Expression of a *Desulfovibrio* tetraheme cytochrome *c* in *Escherichia coli*. 2000. *Biochemical & Biophysical Research Communications* 268: 688-691.

Deshmukh, M., G. Brasseur, and F. Daldal. 2000. Novel *Rhodobacter capsulatus* genes required for the biogenesis of various *c*-type cytochromes. *Molecular Microbiology* 35: 123-138.

Dolla, A., B. K. J. Pohorelic, J. K. Voordouw, and G. Voordouw. 2000. Deletion of the hmc operon of *Desulfovibrio vulgaris* subsp. Hildenborough hampers hydrogen metabolism and low-redox potential niche establishment. *Archives of Microbiology*: 143-151.

Dolla, A., P. Arnoux, I. Protasevich, V. Lobachov, M. Brugna, M. T. Giudici-Orticoni, R. Haser, M. Czjzek, A. Makarov, and M. Bruschi. 1999. Key role of phenylalanine 20 in cytochrome c_3: Structure, stability, and function studies. *Biochemistry* 38: 33-41.

Dolla, A., L. Florens, M. Bruschi, I. V. Dudich, and A. A. Makarov. 1995. Drastic influence of a single heme axial ligand replacement on the thermostability of cytochrome c_3. *Biochemical and Biophysical Research Communications* 211: 742-747.

Dolla, A., L. Florens, P. Bianco, J. Haladjian, G. Voordouw, E. Forest, J. Wall, F. Guerlesquin, and M. Bruschi. 1994. Characterization and oxidoreduction properties of cytochrome after heme axial ligand replacements c_3. *Journal of Biological Chemistry* 269: 6340-6346.

Dolla, A., F. Guerlesquin, M. Bruschi, and R. Haser. 1991. Ferredoxin electron transfer site on cytochrome c_3 structural hypothesis of an intramolecular electron transfer pathway within a tetra-heme cytochrome. *Journal Molecular Recognition* 4: 27-33.

Fabianek, R. A., H. Hennecke, and L. Thony-Meyer. 2000. Periplasmic protein thiol: disulfide oxidoreductases of *Escherichia coli*. *FEMS Microbiology Reviews* 24: 303-316.

Fabianek, R. A., H. Hennecke, and L. Thony-Meyer. 1998. The active-site cysteines of the periplasmic thioredoxin-like protein CcmG of *Escherichia coli* are important but not essential for cytochrome *c* maturation in vivo. *Journal of Bacteriology* 180: 1947-1950.

Feng, Y., R. P. Swenson. 1997. Evaluation of the role of specific acidic amino acid residues in electron transfer between the flavodoxin and cytochrome c_3 from *Desulfovibrio vulgaris. Biochemistry* 44: 13617-13628.

Ganesh, R., K. G. Robinson, G. D. Reed, and G. S. Sayler. 1997. Reduction of Hexavalent Uranium from Organic Complexes by Sulfate- and Iron-Reducing Bacteria. *Applied & Environmental Microbiology* 63: 4385-4391.

Goldman, B. S., D. L. Beckman, A. Bali, E. M. Monika, K. K. Gabbert, and R. G. Kranz. 1997. Molecular and immunological analysis of an ABC transporter complex required for cytochrome *c* biogenesis. *Journal of Molecular Biology* 268: 724-738.

Goldman, B. S., D. A. Sherman, and R. G. Kranz. 1997. Comparison of the bacterial hela protein to the f508 region of the cystic fibrosis transmembrane regulator. *Journal of Bacteriology* 179: 7869-7871.

Goodhew, C. F., K. R. Brown, and G. W. Pettigrew. 1986. Haem Staining in Gels, A Useful Tool in the Study of Bacterial *c*-type Cytochromes. *Biochimica et Biophysica Acta*: 288-294.

Hamilton, W. A. 1985. Sulphate-reducing bacteria and anaerobic corrosion. *Annual Review of Microbiology*: 195-217.

Heidelberg, J. F., R. Seshadri, S. A. Haveman, C. L. Hemme, I. T. Paulsen, J. F. Kolonay, J. A. Eisen, N. Ward, B. Methe, L. M. Brinkac, S. C. Daugherty, R. T. Deboy, R. J. Dodson, A. S. Durkin, R. Madupu, W. C. Nelson, S. A. Sullivan, D. Fouts, D. H. Haft, J. Selengut, J. D. Peterson, T. M. Davidsen, N. Zafar, L. W. Zhou, and D. Radune. 2004. The genome sequence of the anaerobic, sulfate-reducing bacterium *Desulfovibrio vulgaris* Hildenborough. *Nature Biotechnology* 22: 554-559.

Katzen, F., and J. Beckwith. 2000. Transmembrane electron transfer by the membrane protein DsbD occurs via a disulfide bond cascade. *Cell* 103: 769-779.

Kredich, N. M. 1996. Biosynthesis of Cysteine. Pages 514-527. *Eschericia coli and Salmonella Cellular and Molecular Biology*.

Londer, Y. Y., P. R. Pokkuluri, D. M. Tiedi, and M. Schiffer. 2002. Production and preliminary characterization of recombinant triheme cytochrome c_7 from *Geobacter sulfurreducens* in *Escherichia coli*. *Biochimica et Biophysica Acta* 1554: 202-211.

Lovley, D. R. 1993. Dissimilatory Metal Reduction. *Annual Review of Microbiology*: 263-290.

Lovley, D. R., P. K. Widman, J. C. Woodward, and E. J. P. Phillips. 1993. Reduction of uranium by cytochrome-c(3) of *Desulfovibrio vulgaris*. *Applied & Environmental Microbiology* 59: 3572-3576.

Mitchell, P., and J. Moyle. 1965. Evidence discriminating between the chemical and chemiosmotic mechanisms of electron transport phosphorylation. *Nature*: 1205-1206.

Mus-Veteau, I., A. Dolla, F. Guerlesquin, F. Payan, M. Czjzek, R. Haser, P. Bianco, J. Haladjian, B. J. Rapp-Giles, and J. D. Wall. 1992. Site-directed mutagenesis of tetraheme cytochrome c_3 Modification of oxidoreduction potentials after heme axial ligand replacement. *Journal of Biological Chemistry* 267: 16851-16858.

Noguera, D. R., G. A. Brusseau, B. E. Rittmann, and D. A. Stahl. 1998. A unified model describing the role of hydrogen in growth of *Desulfovibrio vulgaris* under different environmental conditions. *Biotechnological Bioengineering*: 732-746.

Odom, J. M. 1993. Industrial and Environmental Activities of Sulfate-Reducing Bacteria. Pages 159-210 in J. M. S. Odom, R., ed. *The Sulfate-Reducing Bacteria: Contemporary Perspectives*. Springer-Verlag, New York.

Odom, J. M., and H. D. J. Peck. 1981. Hydrogen Cycling as a General Mechanism for Energy Coupling in the Sulfate-Reducing Bacteria, *Desulfovibrio* sp. *FEMS Microbiology Letters*: 47-50.

Ozawa, K., Y. Takayama, F. Yasukawa, T. Ohmura, M. A. Cusanovich, Y. Tomimoto, H. Ogata, Y. Higuchi, and H. Akutsu. 2003. Role of the aromatic ring of Tyr43 in tetraheme cytochrome c_3 from *Desulfovibrio vulgaris* Miyazaki F. *Biophysical Journal* 85: 3367-3374.

Page, M. D., D. A. Pearce, H. A. C. Norris, and S. J. Ferguson. 1997. The *Paracoccus denitrificans ccma*, *b* and *c* genes - cloning and sequencing, and analysis of the potential of their products to form a haem or apo- c-type cytochrome transporter. *Microbiology* 143: 563-576.

Pattarkine, M., J. J. Tanner, Y. -H. Lee, and J. D. Wall. *Desulfovibrio desulfuricans* G20 tetraheme cytochrome structure at 1.5 Å and cytochrome interaction with metal complexes. Manuscript in preparation.

Payne, R. B., D. A. Gentry, B. J. Rapp-Giles, L. Casalot, and J. D. Wall. 2002. Uranium reduction by *Desulfovibrio desulfuricans* strain G20 and a cytochrome c_3 mutant. *Applied & Environmental Microbiology* 68: 3129-3132.

Pereira, A. S., I. Pacheco, M.-Y. Liu, J. Legall, A. V. Xavier, and M. Tereira. 1997. Multiheme cytochromes from the Sulfur-reducing bacterium *Desulfuromonas acetoxidans*. *European Journal of Biochemistry* 248: 323-328.

Pohorelic, B. K. J., J. K. Voordouw, E. Lojou, A. Dolla, J. Harder, and G. Voordouw. 2002. Effects of Deletion of Genes Encoding Fe-Only Hydrogenase of *Desulfovibrio vulgaris* Hildenborough on Hydrogen and Lactate Metabolism. *Journal of Bacteriology*: 679-686.

Postgate, J. 1984. *The Sulfate-Reducing Bacteria*. Cambridge University Press, Cambridge.

Program, N. A. B. I. R. 2003. Bioremediation of Metals and Radionuclides: What It Is and How It Works. Office of Biological and Environmental Research, Office of Science, U.S. Department of Energy.

Rapp-Giles, B. J., L. Casalot, R. S. English, J. A. Ringbauer, Jr., A. Dolla, and J. D. Wall. 2000. Cytochrome c_3 mutants of *Desulfovibrio desulfuricans*. *Applied & Environmental Microbiology* 66: 671-677.

Rapp, B. J., and J. D. Wall. 1987. Genetic Transfer in *Desulfovibrio desulfuricans*. *Proceeding of the National Academy of Science U S A*: 9128-9130.

Reid, E., J. Cole, and D. J. Eaves. 2001. The *Escherichia coli* CcmG protein fulfils a specific role in cytochrome c assembly. *Biochemical Journal* 355: 51-58.

Reid, E., D. J. Eaves, and J. A. Cole. 1998. The CcmE protein from *Escherichia coli* is a haem-binding protein. *FEMS Microbiology Letters* 166: 369-375.

Ren, Q., U. Ahuja, and L. Thony-Meyer. 2002. A bacterial cytochrome *c* heme lyase CcmF forms a complex with the heme chaperone CcmE and CcmH but not with apocytochrome c. *Journal of Biological Chemistry* 277: 7657-7663.

Ren, Q., and L. Thony-Meyer. 2001. Physical interaction of CcmC with heme and the heme chaperone CcmE during cytochrome c maturation. *Journal of Biological Chemistry* 276: 32591-32596.

Rousset, M., L. Casalot, B. J. Rapp-Giles, Z. Dermoun, P. de Philip, J. P. Belaich, and J. D. Wall. 1998. New shuttle vectors for the introduction of cloned DNA in *Desulfovibrio*. *Plasmid* 39: 114-122.

Salgueiro, C. A., P. N. da Costa, D. L. Turner, A. C. Messias, W. M. van Dongen, L. M. Saraiva, and A. V. Xavier. 2001. Effect of hydrogen-bond networks in controlling reduction potentials in *Desulfovibrio vulgaris* (Hildenborough) cytochrome c_3 probed by site-specific mutagenesis. *Biochemistry* 40: 9709-9716.

Saraiva, L. M., C. A. Salgueiro, P. N. da Costa, A. C. Messias, J. LeGall, W. M. van Dongen, and A. V. Xavier. 1998. Replacement of lysine 45 by uncharged residues modulates the redox-Bohr effect in tetraheme cytochrome c_3 of *Desulfovibrio vulgaris* (Hildenborough). *Biochemistry* 35: 12160-12165.

Schulz, H., R. A. Fabianek, E. C. Pellicioli, H. Hennecke, and L. Thony-Meyer. 1999. Heme transfer to the heme chaperone CcmE during cytochrome c maturation requires the CcmC protein, which may function independently of the ABC-transporter CcmAB. *Proceedings of the National Academy of Sciences of the United States of America* 96: 6462-6467.

Schulz, H., H. Hennecke, and L. Thonymeyer. 1998. Prototype of a heme chaperone essential for cytochrome *c* maturation. *Science* 281: 1197-1200.

Schulz, H., E. C. Pellicioli, and L. Thony-Meyer. 2000. New insights into the role of CcmC, CcmD and CcmE in the heme delivery pathway during cytochrome *c* maturation by a complete mutational analysis of the conserved tryptophan-rich motif of CcmC. *Molecular Microbiology* 37: 1379-1388.

Schulz, H., and L. Thony-Meyer. 2000. Interspecies complementation of *Escherichia coli* ccm mutants: CcmE (CycJ) from *Bradyrhizobium japonicum* acts as a heme chaperone during cytochrome *c* maturation. *Journal of Bacteriology* 182: 6831-6833.

Spielewoy, N., H. Schulz, J. M. Grienenberger, L. Thony-Meyer, and G. Bonnard. 2001. CcmE, a nuclear-encoded heme-binding protein involved in cytochrome *c* maturation in plant mitochondria. *Journal of Biological Chemistry* 276: 5491-5497.

Takayama, Y., E. Harada, R. Kobayashi, K. Ozawa, and H. Akutsu. 2004. Roles of noncoordinated aromatic residues in redox regulation of cytochrome c_3 from *Desulfovibrio vulgaris* Miyazaki F. *Biochemistry* 43: 10859-10866.

Thomas, P. E., D. Ryan, and W. Levin. 1976. An Improved Staining Procedure for the Detection of the Peroxidase Activity of Cytochrome P-450 on Sodium Dodecyl Sulfate Polyacrylamide Gels. *Analytical Biochemistry*: 168-176.

Thony-Meyer, L. 2000. Heme-polypeptide interactions during cytochrome *c* maturation. *Biochimica et Biophysica Acta* 1459: 316-324.

Thony-Meyer, L., and P. Kunzler. 1997. Translocation to the periplasm and signal sequence cleavage of preapocytochrome *c* depend on sec and lep, but not on the ccm gene products. *European Journal of Biochemistry* 246: 794-799.

Van den Berg, W. A., J. P. Stokkermans, and W. M. Van Dongen. 1989. Development of a plasmid transfer system for the anaerobic sulphate reducer, *Desulfovibrio vulgaris* (Hildenborough) genome. *Journal of Biotechnology* 12: 173-184.

Van Der Westen, H., S. G. Mayhew, and C. Veeger. 1978. Separation of hydrogenase from intact cells of *Desulfovibrio vulgaris*. *FEBS Letters* 86: 122-126.

Von Wolzogen Kuhr, C. A. H., and I. S. van der Vulgt. 1934. The graphitization of cast iron as an electrobiochemical process in anaerobic soils. *Water*: 147-165.

Voordouw, G., W. B. Pollock, M. Bruschi, F. Guerlesquin, B. J. Rapp-Giles, and J. D. Wall. 1990. Functional expression of *Desulfovibrio vulgaris* Hildenborough cytochrome c_3 in *Desulfovibrio desulfuricans* G200 after conjugational gene transfer from *Escherichia coli*. *Journal of Bacteriology* 172: 6122-6126.

Wall, J. D., B. J. Rapp-Giles, and M. Rousset. 1993. Characterization of a small plasmid from *Desulfovibrio desulfuricans* and its use for shuttle vector construction. *Journal of Bacteriology* 175: 4121-8.

Weimer, P. J., M. J. Van Kavelaar, C. B. Michel, and T. K. Ng. 1988. Effect of Phosphate on the Corrosion of Carbon Steel and on the Composition of Corrosion Products in Two-Stage Continuous Cultures of *Desulfovibrio desulfuricans*. *Applied & Environmental Microbiology* 54: 386-396.

Widdel, F. 1988. *Microbiology and Ecology of Sulfate- and Sulfur-Reducing Bacteria*. Wiley, New York.

Zhou, Z. and R. P. Swenson. 1995. Electrostatic effects of surface acidic amino acid residues on the oxidation-reduction potentials of the flavodoxin from *Desulfovibrio vulgaris* (Hildenborough). *Biochemistry* 34: 3183-3192.